Department of Theoretical Physics, Faculty of Fundamental Problems of Technology
Wrocław University of Technology

Self-report

Katarzyna Roszak

Wrocław, September 16, 2015

Contents

1 Name **3**

2 Education and degrees **3**

3 Information on previous employment **3**

4 Scientific achievement being the basis of the habilitation procedure **3**
4.1 Title . . . 3
4.2 List of publications constituting the scientific achievement . . . 3
4.3 Description of the scientific goal and the obtained results contained in a the group of research papers presented here as a scientific achievement . . . 4
4.3.1 Introduction . . . 4
4.3.2 Self-assembled QDs versus electrostatically defined QDs . . . 5
4.3.3 Spin and charge qubits in QDs . . . 5
4.3.4 Decoherence . . . 6
4.3.5 Quantum correlations . . . 14
4.3.6 QPC measurement of double QD spin states and phonons . . . 23
4.3.7 Summary . . . 28

5 Description of other scientific achievements **33**
5.1 Bibliometric data (from the 8th of September 2015) . . . 33
5.2 List of articles not included in the habilitation thesis . . . 33
5.2.1 Before obtaining the PhD . . . 33
5.2.2 After obtaining the PhD (articles not included in the habilitation) . . . 33
5.3 Description of the research conducted before obtaining the PhD . . . 34
5.4 Description of the research conducted after obtaining the PhD, which is not included in the habilitation . . . 35
5.5 Awards . . . 35
5.6 Head Investigator in the following grants . . . 35
5.7 Participation in research projects . . . 35
5.8 Invited conference talks . . . 36
5.9 Other conference talks . . . 37

6 International and national collaboration **37**

1 Name

Katarzyna Roszak

2 Education and degrees

2008 PhD in Theoretical Physics,
Institute of Physics, Wrocław University of Technology
Dissertation title: Zaburzenia fononowe stanów ładunkowych i spinowych w kropkach kwantowych
Advisor: prof. dr hab. P. Machnikowski

2004 MSc in Physics,
Faculty of Fundamental Problems of Technology, Wrocław University of Technology
Dissertation title: Dekoherencja informacji kwantowej w technologii kropek kwantowych
Advisor: prof. dr hab. P. Machnikowski

3 Information on previous employment

2004-2008 PhD student at the Institute of Physics,
Wrocław University of Technology

2006-2007 DAAD research scholarship at the Münster University
(in the group of prof. T. Kuhna)

2008-2010 research assistant at the Institute of Physics,
Wrocław University of Technology

2009-2010 postdoctoral position at the Faculty of Mathematics and Physics,
Charles University in Prague(in the group of dr T. Novotný)

2010-2014 specialist position at the Institute of Physics,
Wrocław University of Technology

2014 postdoctoral position at the Faculty of Mathematics and Physics,
Charles University in Prague (June-September,
in the group of dr T. Novotný)

2014-now adiunkt at the Department of Theoretical Physics,
Wrocław University of Technology

4 Scientific achievement being the basis of the habilitation procedure

The scientific achievement, in acordance with the art. 16 paragraph 2 of the Act of March 14th, 2003, concerning scientific degrees and titles (Dz. U. no. 65, item 595, as amended), is the series of publications entitled:

4.1 Title

"The impact of the environment on the coherence and quantum correlations of quantum dot ensambles"

4.2 List of publications constituting the scientific achievement

[H1] K. Roszak, P. Machnikowski, *Phonon-induced dephasing of singlet-triplet superpositions in double quantum dots without spin-orbit coupling*, Phys. Rev. B **80** (2009) 195315.

[H2] K. Roszak, P. Horodecki, R. Horodecki, *Sudden death of effective entanglement*, Phys. Rev. A **81** (2010) 042308.

[H3] K. Roszak, P. Mazurek, P. Horodecki, *Anomalous decay of quantum correlations of quantum-dot qubits*, Phys. Rev. A **87** (2013) 062308.

[H4] Ł. Marcinowski, K. Roszak, P. Machnikowski, M. Krzyżosiak, *Phonon influence on the measurement of spin states in double quantum dots using the quantum point contact*, Phys. Rev. B **88** (2013) 125303.

[H5] P. Mazurek, K. Roszak, R. W. Chhajlany, P. Horodecki, *Sensitivity of entanglement decay of quantum-dot spin qubits to the external magnetic field*, Phys. Rev. A **89** (2014) 062318.

[H6] P. Mazurek, K. Roszak, P. Horodecki, *The decay of quantum correlations between quantum dot spin qubits and the characteristics of its magnetic-field dependence*, EPL **107** (2014) 67004.

[H7] K. Roszak, Ł. Marcinowski, P. Machnikowski, *Decoherence-enhanced quantum measurement of a quantum-dot spin qubit*, Phys. Rev. A **91** (2015) 032118.

[H8] K. Roszak, R. Filip, T. Novotný, *Decoherence control by quantum decoherence itself*, Sci. Rep. **5** (2015) 9796.

4.3 Description of the scientific goal and the obtained results contained in a the group of research papers presented here as a scientific achievement

4.3.1 Introduction

The described scientific achievement involves the study a number of realistic scenarios involving QDs (QDs) which are of interest both from the point of view of our understanding of quantum mechanics and of potential experimental realizations of devices utilizing coherence of QD states. The approach allowed me to characterize the possible evolution of quantum correlations in QD systems (described by both quantum entanglement and the quantum discord, which prove to have different regimes of usefulness for e. g. magnetic field measurement) and specify the means and limitations for the experimental characterization of entanglement, both for spin and exciton qubits. For singlet-triplet spin qubits, which are protected against decoherence from the hyperfine interaction with the spins of atomic nuclei, I found a phononic decoherence mechanism which relies on the Pauli exclusion principle but does not require the spin-orbit coupling and which is dominant at very low temperatures. Using a similar approach, I was able to characterize the effect of decoherence on a proposed measurement scenario of these singlet-triplet qubits and find a situation when decoherence is actually desirable an leads to an enhanced distinguishability of a quantum projective measurement.

Quantum dots. Quantum dots (QDs) [1, 2], zero-dimensional nanostructures embedded in the solid state, are very convenient for the study of the effects of decoherence on quantum behavior. This is because, firstly, their small dimensionality practically guarantees a wide range of quantum behavior of the charge and spin states of charge carriers confined in the dots. Secondly, being solid-state systems, QDs are susceptible to different types of decoherence processes due to interactions with the solid-state environment, depending on the QD states in question, and on the type of semiconductor material they are made of. This involves a wide range of phonon-induced effects (interactions with vibrations of the crystal lattice are unavoidable in the solid state), but also other interactions need to be taken into account which result from the presence of the bulk surrounding the QDs.

Furthermore, the zero-dimentionality of QDs, which is responsible for the quantization of confined states in all three dimensions, allows for their simplified, atomic-like, treatment. Although such a simplification may seem (nadmierne) regarding the description of objects which vary in size from a few to hundreds of nanometers (in all three dimensions), and which are in fact composed of thousands of atoms, it has repeatedly proven to be sufficient to yield both qualitatively and quantitatively valid results. The advantage of such a treatment lies, apart from saving computational time, in the fact that the obtained results can often be found in an almost analytical form (up to the dependence on the actual size and shape of QDs, when numerical treatment is necessary). Although in many situations such a semi-analytical treatment is fairly irrelevant, in the study of the evolution of quantum correlations (and up to a certain level, the study of quantum decoherence) a deeper understanding of the physics underlying the observed processes often depends on obtaining such semi-analytical mathematical formulas for the description of the evolution, and therefore a simplified description of the quantum information characteristics studied.

4.3.2 Self-assembled QDs versus electrostatically defined QDs

Many different systems have been described as QDs, the most exotic of which are colloidal QDs, which are in fact nanocrystals suspended in liquid and graphene flakes. The common factor for structures described as QDs is a discrete structure of the (few) energy levels which leads to an energy spectrum which resembles that of atoms. Here, I limit myself to two types of semiconductor QDs which are in fact examples of three dimensional quantum wells embedded in a solid state environment.

The first type are called self-assembled QDs [3, 4, 5] and they are formed of a small island of one semiconductor material inside of a different semiconductor material. These kind of dots form spontaneously, if the lattice constant of the two semiconducting crystals vary by a small amount. Then, when the QD material is grown on a crystal surface of the material in which the QD is embedded, the strain resulting from the mismatch of the lattice constants lead to the formation of islands instead of the first few layers. If the growth is then stopped, an irregular array of QDs is obtained. The sizes and density of the dots depends not only on the growth parameters, but also on the materials used. An advantage of self-assembled QDs is the fact that again due to strain, QDs in different layers tend to nucleate on top of one another, leading to naturally occurring double QDs or even stacks of a few quantum dots.

Self-assembled QDs are most commonly used in experiments where the qubit manipulation is performed optically. These can involve both charge and spin states, although the optical manipulation of the spin of single charge carriers (electrons or holes) often requires the utilization of spin states of a larger number of particles (such as trions). In the following, whenever excitonic qubits are discussed, material and dot parameters which are used correspond to self-assembled GaAs/InGaAs QDs.

The second type of QDs discussed here are called electrostatically defined or lateral QDs [6, 7, 8]. These are formed in two-dimensional electron gas (2DEG) by embedding (almost circular) leads on top of a two-dimensional quantum well. Gate voltages applied to the leads restrict the movement of electrons in the 2DEG the two remaining dimensions forming the QDs. These type of dots are usually used in any experiments which involve electric control of quantum states, most significantly experiments on spin qubits.

4.3.3 Spin and charge qubits in QDs

Solid state systems are sought after for quantum information processing, since they should be easier to integrate with existing computers and promise to be more robust than other ensembles. Different QD states have been proposed as potential qubits for solid state quantum information processing. These can be broadly divided into charge and spin qubits, which differ

most substantially when it comes to initialization techniques, the possibilities of manipulation and measurement, as well as the decoherence processes to which they are susceptible.

A range of charge carriers which can occupy a QD and the limit to their number differs depending on the size of the dot. Although the basic particles to be confined are limited to electrons and holes, already an exciton (interacting electron-hole pair) requires a different experimental and theoretical treatment than the electron and the hole alone. Foremost, an exciton can be excited optically in an empty QD via the transfer of an electron from the valence band into the conduction band, which is impossible for either the electron or the hole alone. In the following excitonic qubits [9], for which the qubit state $|0\rangle$ denotes an empty QD and the qubit states $|1\rangle$ means that the QD is occupied by an electron in its ground state, and their interaction with the phonon environment is broadly discussed.

Spin states are better protected from the environment, but as a trade off, they are also much harder to manipulate. The appeal of long decay and coherence times has lead to the original proposal of a spin qubit [10] which was specified as the spin-up and spin-down state of a single electron confined in a QD. Although this type of qubit is immune to the fast decoherence processes which are mediated by phonons, because the charge state of both qubit states is the same and the spin-orbit interaction is weak, it takes much longer to address than any of the charge qubits. The main decoherence process for such spin qubits is due to the hyperfine interaction between the electron spin and the spins of the nuclei of the atoms of which the QD is formed. This decoherence, although orders of magnitude slower than phonon-induced effects, has as yet been enough to hinder effective quantum information processing on spin qubits.

One of the solutions of the problem of the hyperfine interaction is to use more involved spin states as qubits. The simplest pair of spin states which are protected (by symmetry) from the hyperfine interaction with the environment is the low energy spin-singlet state and the spin-triplet state of two ground-state electrons confined two QDs (which are as identical as possible). The singlet-triplet qubits have the additional advantage that they are more straightforward to prepare and measure in electrostatically defined QDs (through the manipulation of the electrostatic potential of the dots) than single spin qubits. On the other hand, the higher energy singlet states are energetically separated only via the Coulomb interaction which tries to prevent double QD occupation. This opens the way for other decoherence channels than the hyperfine interaction, including phonons.

In the following, both types of spin qubits introduced above are discussed in the context of quantum information processing and magnetic field measurement.

4.3.4 Decoherence [H1, H8]

Decoherence is the principal issue for most types of qubits. In solid state systems it is a particularly valid problem, because there is no way of isolating the qubit from an environment in which it is embedded. From the point of view of coherent quantum applications, two kinds of decoherence are of interest. One is spin relaxation (thermalization of occupations) between the selected basis states (qubit states). The other one is dephasing of superpositions made of these states. Such a process, often referred to as pure dephasing, does not affect the occupations of the qubit basis states, thus conserving the classical information of the system. However, by destroying quantum coherence, it degrades the quantum bit to a classical one and hence is detrimental for quantum information storage or processing. Moreover, if the system is initially prepared in a superposition of the basis states, the pure dephasing process will lead to a decay of this state.

The most prominent sources of decoherence for QDs are the interaction with phonons and the hyperfine interaction (the latter is important only for spin qubits). In what follows, I will introduce examples of decoherence which results from both kinds of interactions. The choice is dictated by the relevance of the decoherence processes to the scientific achievement which is

being presented.

Phonon-induced decoherence of an excitonic qubit. The phonon-induced decoherence of a superposition state of an excitonic qubit (introduced in Sec. 4.3.3), is be dominated by the deformation potential coupling [ksiazka,krummheuer02]. This results from the fact that the piezoelectric coupling is directly related to the Coulomb interaction between the confined charge distribution and the phonon-related polarization field. For an electron and a hole localized in the same spatial volume with strongly overlapping wavefunctions there will be a large cancellation effect between the piezoelectric interaction of the two charged particles.

The resulting decoherence takes the form of partial pure dephasing [11, 12, 13]. Pure dephasing means that the occupation of the dot remains unchanged while the phase information of the quantum dot state leaks into the environment, reducing the amplitude of the off-diagonal elements of the density matrix. The partiality, which is due to the super-Ohmic character of the phonon environment, on the other hand means that the process is not exponential and a finite amount of coherence is left in the superposition state even at long times.

The Hamiltonian of the system is given by

$$H = \epsilon|1\rangle\langle 1| + \sum_{\boldsymbol{k}} \hbar\omega_{\boldsymbol{k}} b^\dagger_{\boldsymbol{k}} b_{\boldsymbol{k}} + |1\rangle\langle 1| \sum_{\boldsymbol{k}} (f^*_{\boldsymbol{k}} b_{\boldsymbol{k}} + f_{\boldsymbol{k}} b^\dagger_{\boldsymbol{k}}), \tag{1}$$

where the first term describes the energy of the confined exciton (ϵ is the energy difference between the states without phonon corrections), the second term is the Hamiltonian of the phonon subsystem and the third term describes the interaction. Carrier-phonon interaction constants in (1) are given by

$$f_{\boldsymbol{k}} = (\sigma_{\mathrm{e}} - \sigma_{\mathrm{h}}) \sqrt{\frac{\hbar k}{2\varrho V_{\mathrm{N}} c}} \int_{-\infty}^{\infty} d^3\boldsymbol{r} \psi^*(\boldsymbol{r}) e^{-i\boldsymbol{k}\cdot\mathrm{r}} \psi(\boldsymbol{r}), \tag{2}$$

and describe the deformation potential coupling between the carriers and the lattice modes. Here ϱ is the crystal density, V_{N} is the normalization volume of the phonon system, $\omega_{\boldsymbol{k}} = ck$ is the frequency of the phonon mode with the wave vector $\boldsymbol{k}$ (c is the speed of longitudinal sound), and $b^\dagger_{\boldsymbol{k}}$, $b_{\boldsymbol{k}}$ are phonon creation and annihilation operators.

The carrier-phonon interaction term in Eq. (1) is linear in phonon operators and describes a shift of the lattice equilibrium induced by the presence of a charge distribution in the dot. The stationary state of the system corresponds to the exciton and the surrounding coherent cloud of phonons representing the lattice distortion to the new equilibrium. The transformation that creates the coherent cloud is the shift $w b_{\boldsymbol{k}} w^\dagger = b_{\boldsymbol{k}} - f_{\boldsymbol{k}}/(\hbar\omega_{\boldsymbol{k}})$, generated by the Weyl operator [D4]

$$w = \exp\left[\sum_{\boldsymbol{k}} \left(\frac{f_{\boldsymbol{k}}}{\hbar\omega_{\boldsymbol{k}}} b^\dagger_{\boldsymbol{k}} - \frac{f^*_{\boldsymbol{k}}}{\hbar\omega_{\boldsymbol{k}}} b_{\boldsymbol{k}} \right)\right]. \tag{3}$$

A straightforward calculation shows that the Hamiltonian (1) is diagonalized by the unitary transformation $\mathbb{W} = |0\rangle\langle 0| \otimes \mathbb{I} + |1\rangle\langle 1| \otimes w$, where $\mathbb{I}$ is the identity operator and the tensor product refers to the carrier subsystem (first component) and its phonon environment (second component).

Following Ref. [D4] we can find the exact time-evolution of the QD density matrix under the perturbation of a phonon bath. For a pure (fully coherent) initial state

$$|\psi\rangle = a|0\rangle + b|1\rangle \tag{4}$$

this is

$$\rho(t) = \begin{pmatrix} |a|^2 & a^* b e^{iEt/\hbar} \langle W(t)\rangle \\ ab^* e^{-iEt/\hbar} \langle W^\dagger(t)\rangle & |b|^2 \end{pmatrix}, \tag{5}$$

where $E = \epsilon - \sum_{\boldsymbol{k}} |f_{\boldsymbol{k}}|^2/(\hbar\omega_{\boldsymbol{k}})$ is the shifted exciton energy and the average of Weyl operators at thermal equilibrium is equal to

$$\langle W(t)\rangle = \langle w^\dagger(t)w\rangle = \exp\left[-i\sum_{\boldsymbol{k}}\left|\frac{f_{\boldsymbol{k}}}{\hbar\omega_{\boldsymbol{k}}}\right|^2 \sin\omega_{\boldsymbol{k}}t\right] \times \exp\left[\sum_{\boldsymbol{k}}\left|\frac{f_{\boldsymbol{k}}}{\hbar\omega_{\boldsymbol{k}}}\right|^2 (\cos\omega_{\boldsymbol{k}}t - 1)(2n_{\boldsymbol{k}}+1)\right];$$

$n_{\boldsymbol{k}}$ are bosonic equilibrium occupation numbers.

In the case of two qubits interacting with the same phonon environment the system is described by the Hamiltonian

$$\begin{aligned} H &= \epsilon_1(|1\rangle\langle 1|\otimes\mathbb{I}) + \epsilon_2(\mathbb{I}\otimes|1\rangle\langle 1|) + \Delta\epsilon(|1\rangle\langle 1|\otimes|1\rangle\langle 1|) + (|1\rangle\langle 1|\otimes\mathbb{I})\sum_{\boldsymbol{k}} f_{\boldsymbol{k}}^{(1)}(b_{\boldsymbol{k}}^\dagger + b_{-\boldsymbol{k}}) \\ &\quad +(\mathbb{I}\otimes|1\rangle\langle 1|)\sum_{\boldsymbol{k}} f_{\boldsymbol{k}}^{(2)}(b_{\boldsymbol{k}}^\dagger + b_{-\boldsymbol{k}}) + \sum_{\boldsymbol{k}}\omega_{\boldsymbol{k}} b_{\boldsymbol{k}}^\dagger b_{\boldsymbol{k}}. \end{aligned} \tag{6}$$

This Hamiltonian is composed of two single qubit Hamiltonians of Eq. (1) (where the energies and the coupling constants of the two dots are distinguished by the indices 1 and 2) and an additional interaction term which describes the energy shift which is present when both dots are occupied (the biexcitonic shift), $\Delta\epsilon$. The coupling constants for identical QDs have the form $f_{\boldsymbol{k}}^{(1,2)} = f_{\boldsymbol{k}} e^{\pm ik_z d/2}$, where $f_{\boldsymbol{k}}$ is given by Eq. (2) and d is the distance between the dots. The Hamiltonian (6) is diagonalized by an analogous Weyl transformation as in the single qubit case and the evolution of the QD density matrix can be found in a straightforward manner by a generalization of the single qubit results.

A scheme for minimizing phonon decoherence of an excitonic qubit [H8]. The creation of an exciton in a superposition state in the solid state environment of a QD perturbs the surrounding crystal lattice and hence, leads to a modification of the state of the phonon environment. Thus, it is logical to assume that applying repeated measurements in the basis corresponding to the initial QD state (which is analogous to the quantum Zeno effect) will not only freeze the QD evolution for the duration of the measurements, but will also affect the degree of partial pure dephasing resulting from the carrier-phonon interaction.

The measurement on the QD subsystem is taken into account as a projection measurement in the quantum-mechanical sense (as opposed to a realistic optical measurement which is natural in this system). We are hence dealing with projection operators of the form

$$P_+ = |\psi\rangle\langle\psi|\otimes\mathbb{I}, \tag{7}$$

$$P_- = |\psi_\perp\rangle\langle\psi_\perp|\otimes\mathbb{I}, \tag{8}$$

with $|\psi\rangle$ equal to the initial state given by Eq. (4) and the perpendicular $|\psi_\perp\rangle = b^*|0\rangle - a^*|1\rangle$ (the unity $\mathbb{I}$ is in the phonon subsystem). Note, that regardless of the measurement outcome the degree of coherence is retained and equal to one at the time of the last measurement ($D(t) = |\langle 0|\rho(t)|1\rangle|/|a^*b|$), so that an outcome of $|\psi_\perp\rangle$ is not necessarily unfavorable.

The degree of coherence at any given time may be calculated using a recursive scheme given the state of the reservoir at the last measurement time, $D(t) = |\langle W(t-\tilde{\tau})\rangle_n|$. Here $\tilde{\tau} = \sum_{m=1}^n \tau_m$ is the sum of all delay times between the n measurements that occurred until time t, and $\langle ...\rangle_n$ denotes the average over the reservoir degrees of freedom, with the reservoir state at the time of the n-th measurement $R(\tilde{\tau})$. The state of the reservoir at the time of the last measurement $\tilde{\tau}$ can be found, if the state of the reservoir after the one-but-last measurement is known (it depends on the measurement outcome). For the explicit form of $R(\tilde{\tau})$ see Ref. [H8].

The left panel of Fig. 1 shows the maximal and minimal long-time values (asymptotic) of the degree of coherence (D_∞) as a function of the delay time. As can be seen the gain (or loss) stabilizes at a given level, if the delay time is longer than a few-picosecond threshold value that corresponds to the time after initialization when the maximal partial pure dephasing is reached.

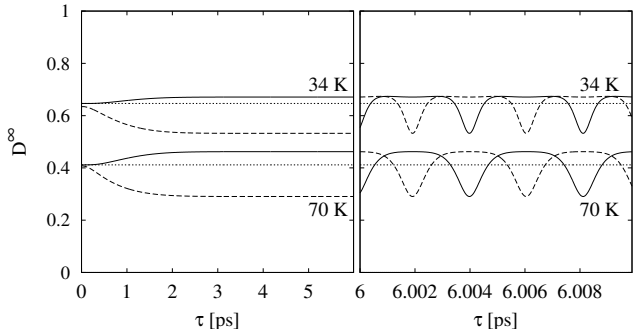

Figure 1: Asymptotic degree of coherence as a function of the delay time for two temperatures. The maximal (solid line) and minimal (dashed line) values are shown in the left panel. The right panel shows the detail for the measurement outcome $|\psi\rangle$ (solid line) and $|\psi_\perp\rangle$ (dashed line). The dotted lines denote the degree of coherence in the case of no extra measurement in both panels.

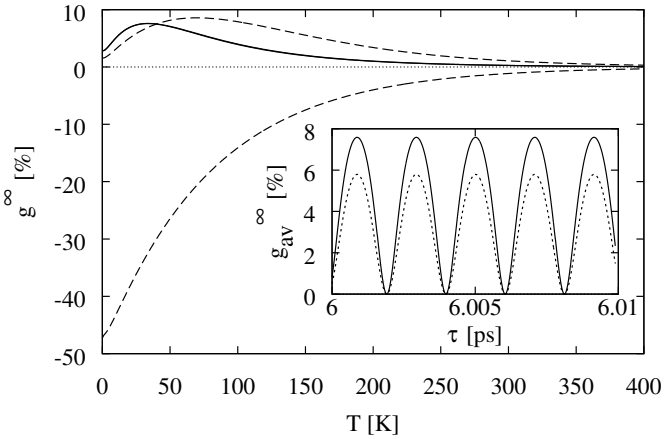

Figure 2: Temperature dependence of the gain in the asymptotic degree of coherence after single measurement. Dashed lines correspond to the point of maximal gain ($E\tau = 2\pi j$) for the measurement outcomes $|\psi\rangle$ (gain) and $|\psi_\perp\rangle$ (loss). The solid line corresponds to the point of equal gain ($E\tau = (j + 1/2)\pi$).

In the right panel in the same figure the full dynamics is shown. The oscillations arize from the interplay of the coherent-QD-evolution-dependent terms which are present in the reservoir state due to the measurement and the actual QD evolution.. The minima (maxima) for the measurement outcome $|\psi\rangle$ ($|\psi_\perp\rangle$) correspond to the situation when $E\tau = (2j + 1)\pi$ (point of minimal gain) and the maxima (minima) to $E\tau = 2\pi j$ (point of maximal gain), where j is a natural number (?). A higly interesting point is at $E\tau = (j+1/2)\pi$ when the gain in coherence is equal for both measurement outcomes (point of equal gain); interestingly this gain is not much different than that at the point of maximal gain and at some temperatures may even be slightly larger (see the 34 K curves).

The temperature dependendce of the gain in the asymptotic degree of coherence, $g_\infty = (D_\infty - D^0_\infty)/(1 - D^0_\infty)$, is shown in Fig. 2. D^0_∞ denotes the asymptotic degree of coherence in the case of no measurement. Surprizingly, the temperature dependence has a maximum and these maxima differ for the different points of gain. The optimal temperature in case of a measurement at the point of maximal gain is $T_m \equiv 70$ K for the material paramters used, while it is around 34 K for the point of equal gain. Note, that for low temperatures the gain at the maximal point is smaller than at the equal point. The loss at minimal point has no extremum and it is proportionally smaller with rising temperature, hence, rising the temperature diminishes the loss in coherence sustained by the wrong measurement outcome at the point of maximal gain (the point of maximal gain for outcome $|\psi\rangle$ corresponds to the minimal gain of outcome $|\psi_\perp\rangle$).

Although the fast oscillations of the asymptotic degree of coherence may suggest potential problems in the experimental realization of the decoherence-reducing scheme, this is not in fact the case. The reason for this is that the probability of measuring outcome $|\psi\rangle$ oscillates synchronously with the degree of coherence around the value of 1/2 ($|a|^4 + |b|^4$). This means that the probability of measuring state $|\psi\rangle$ is maximal when the reduction of dephasing because of the measurement of this state is greatest and likewise for state $|\psi_\perp\rangle$.

Phonon-induced spin decoherence. Spin qubits are typically less prone to decoherence than charge qubits. In QDs this is due to the fact that there is no direct interaction between spins and fonons. Hence, phonon induced processes which affect the spin must relay on a second interaction which couples spin and orbital degrees of freedom of charge carriers confined in QDs. The spin-orbit coupling is such an interaction, but it is usually small which results in the phonon perturbations on the spin state being small as well [14, 15, 16, 17, 18, 19].

Phonon decoherence of spin singlet-triplet qubits [H1] Below an efficient pure dephasing channel which is always present in systems of two electron spins localized in coupled semiconductor QDs is demonstrated. This channel results solely from the charge-phonon interaction in the presence of inter-dot tunnel coupling, and is essentially due to the distinguishability of singlet and triplet states via Pauli-blocking of certain transitions in the triplet case. The key feature of this decoherence process is that it does not require any spin-environment interaction and relies only on the mechanisms (tunnel coupling and the Pauli principle) that are essential for the implementation of quantum gates. In particular, it appears also in materials with negligible spin-orbit and hyperfine couplings and is essentially independent of the magnetic field.

Qualitatively, in the lowest energy state of the two-electron system, each dot is occupied by a single electron. The spin configuration of the system may then be either singlet or triplet. In the former case, the orbital (spatial) wave function is symmetric and a transition to a doubly occupied state is possible [20]. This is forbidden by Pauli exclusion in the triplet configuration with an anti-symmetric orbital part. Such transitions are inefficient at sub-Kelvin temperatures because the doubly occupied state has a higher energy and the occupation of the required phonon states is negligible. However, a two-phonon process is still possible, in which the absorption of a phonon is followed by the re-emission of another one [21, 22]. In such a process, the doubly occupied state is involved only "virtually" and energy conservation requires only that the two phonons have the same energy (that is, the scattering is elastic) but this energy can be arbitrary. Therefore, even at low temperatures, phonons scatter on a double QD in the singlet state, while a double QD in the triplet state is transparent to phonons. In this way, the singlet and triplet states can be distinguished by the macroscopic environment and each scattering event builds up correlation between the spin system and the crystal lattice. This distinguishability leads to pure dephasing of any singlet–triplet superposition, in some sense analogous to the "collisional decoherence" of the orbital degrees of freedom [23, 24]. Although the intensity of this process drops down at low temperatures because of decreasing two-phonon spectral density at low frequencies, the temperature dependence is only polynomial (as opposed to exponential suppression of real transitions). At sub-Kelvin temperatures, at which spin coherent control experiments on double QDs are performed, the two-phonon process can still lead to pure dephasing times as low as tens or hundreds of microseconds.

The Hamiltonian of the system is

$$H = H_{\mathrm{DQD}} + H_{\mathrm{ph}} + H_{\mathrm{int}}. \tag{9}$$

The first term describes the electrons and has the form

$$H_{\mathrm{DQD}} = -t_1 \sum_s \left(a^\dagger_{\mathrm{L}s} a_{\mathrm{R}s} + \mathrm{h.c.} \right) + \frac{1}{2} \sum_{s,s'} \sum_{i,j,k,l} V_{ijkl} a^\dagger_{is} a^\dagger_{js'} a_{ks'} a_{ls}, \tag{10}$$

where $a_{is}, a^\dagger_{is}$ are the electron annihilation and creation operators with $i = \mathrm{L}, \mathrm{R}$ denoting the left and right dot, respectively, and $s = \uparrow, \downarrow$ labeling the spin orientation. The first term in Eq. (**??**) accounts for single-particle inter-dot tunneling. The second term describes the Coulomb interaction, with $V_{ijkl} = V_{jilk} = V_{klij} = V_{lkji}$ (the wave functions may be chosen such that the matrix elements are real). For identical QDs the Coulomb matrix elements are also invariant under the interchange of the dots, L↔R. Among the Coulomb terms, $V_{\mathrm{LRRL}} =$

$V_{\mathrm{RLLR}} \equiv U_1$ and $V_{\mathrm{LLLL}} = V_{\mathrm{RRRR}} \equiv U_2$ are the energies of the singly- and doubly-charged configurations, $V_{\mathrm{LRLR}} = V_{\mathrm{RLRL}} \equiv E_{\mathrm{X}}$ are exchange energies, $V_{\mathrm{LLRR}} = V_{\mathrm{RRLL}} \equiv t_{\mathrm{C2}}$ is the coupling between the doubly-charged configurations, while V_{RLLL} and equivalent terms account for the coupling between the singly- and doubly-charged configurations and will be denoted by t_{C}.

The QD Hamiltonian can be diagonalized analytically and its eigenstates are the three triplet states

$$|(1,1)T_s\rangle = a^\dagger_{\mathrm{L}s} a^\dagger_{\mathrm{R}s}|0\rangle, \quad s =\uparrow,\downarrow, \tag{11a}$$

$$|(1,1)T_0\rangle = \frac{a^\dagger_{\mathrm{L}\uparrow} a^\dagger_{\mathrm{R}\downarrow} - a^\dagger_{\mathrm{R}\uparrow} a^\dagger_{\mathrm{L}\downarrow}}{\sqrt{2}}|0\rangle \tag{11b}$$

with identical eigenenergy $V_{\mathrm{LRRL}} - V_{\mathrm{LRLR}}$. The singlet eigenstates are given by

$$|(-)S\rangle = \frac{1}{\sqrt{2}}\left(|(2,0)S\rangle - |(0,2)S\rangle\right) \tag{12a}$$

$$|S_+\rangle = \frac{1}{\sqrt{1+\xi^2}}[|(+)S\rangle + \xi|(1,1)S\rangle], \tag{12b}$$

$$|S_-\rangle = \frac{1}{\sqrt{1+\xi^2}}[|(1,1)S\rangle - \xi|(+)S\rangle], \tag{12c}$$

where $|(p,q)S\rangle$ is the spin singlet state with p electrons in the left dot and q electrons in the right dot, while $|(+)S\rangle = \left(|(2,0)S\rangle + |(0,2)S\rangle\right)/\sqrt{2}$. The parameter

$$\xi = \frac{2\sqrt{2}t}{U + \sqrt{U^2 + 8t^2}},$$

where $U = V_{LLLL} + V_{LLRR} - V_LRRL - V_{LRLR}$ and $t = \sqrt{2}(V_{RLLL} - t_1)$. The eigenenergies of the singlet states are equal to $E_{(-)S} = V_{LLLL} - V_{LLRR}$ and $E_\pm = \overline{E} \pm \sqrt{U^2 + 8t^2}/2$, where $\overline{E} = (V_{LLLL} + V_{LLRR} + V_{LRRL} + V_{LRLR})/2$. In the small tunneling regime, $t \ll U$, the parameter $\xi \ll 1$ and $|S_+\rangle \approx |(+)S\rangle$, $|S_-\rangle \approx |(1,1)S\rangle$. The two lowest energy states with different spin symmetry (which constitute the qubit) are any triplet state and the singlet state $|S_-\rangle$.

The Hamiltonian of the phonon reservoir is given by

$$H_{\mathrm{ph}} = \sum_{\boldsymbol{k},\lambda} \hbar\omega_{\boldsymbol{k},\lambda} b^\dagger_{\boldsymbol{k},\lambda} b_{\boldsymbol{k},\lambda},$$

where $b_{\boldsymbol{k},\lambda}, b^\dagger_{\boldsymbol{k},\lambda}$ are phonon annihilation and creation operators for a phonon from a branch λ with a wave vector $\boldsymbol{k}$ and $\hbar\omega_{\boldsymbol{k},\lambda}$ are the corresponding energies.

Since we formulate the model in terms of states localized in individual dots the overlap of the corresponding single particle wave functions is negligible and the off-diagonal phonon couplings (transferring the electrons between the dots) vanish. The electron-phonon interaction is therefore described by

$$H_{\mathrm{int}} = \sum_{s,i}\sum_{\boldsymbol{k},\lambda} F^{(\lambda)}_i(\boldsymbol{k}) a^\dagger_{is} a_{is} (b_{\boldsymbol{k},\lambda} + b^\dagger_{-\boldsymbol{k},\lambda}),$$

where $F^{(\lambda)}_{\mathrm{L/R}}(\boldsymbol{k}) = F^{(\lambda)}(\boldsymbol{k}) \exp[\pm i k_x D/2]$ are coupling constants and D is the inter-dot distance. We include the deformation potential and piezoelectric couplings. The coupling constants for the longitudinal and transverse acoustic phonon branches can be found in Refs [25, 2]. Note that since the electron-phonon interaction conserves spin, the singlet states are not coupled by phonon-assisted transitions to the triplet states.

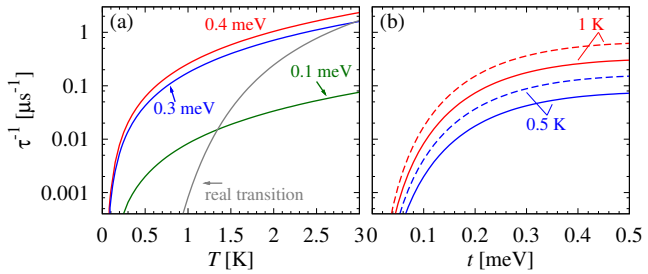

Figure 3: Two-phonon induced pure dephasing rates: (a) As a function of temperature for different tunneling parameters. (b) As a function of the tunneling parameter for different temperatures. Gray line in (a) shows the dephasing rates from single-phonon transitions for $t = 0.3$ meV. All solid lines correspond to $D = 200$ nm, while the dashed lines in (b) show results for $D = 300$ nm.

The evolution of the reduced density matrix of the two-electron subsystem can be described using the time-convolutionless (TCL) projection operator method [26]. For factorized initial conditions (pure initial state), expanding the TCL generator up to the fourth order yields the evolution which accounts for two-phonon-assisted processes which are responsible for the studied effect.

The pure dephasing rates resulting from the two-phonon (scattering) process are shown in Fig. 3(a) as a function of temperature. Dephasing rates due to the single-phonon assisted transition for $t = 0.3$ meV are shown in the same figure for comparison. At low temperatures, at which experiments on double QD ensembles are performed, the single-phonon transition is suppressed. At these temperatures, the dominating decoherence mechanism is the elastic scattering. This two-phonon process is much less influenced by decreasing the temperature since it involves only a virtual transition to a higher energy (doubly charged) singlet state. The resulting pure dephasing rates at sub-Kelvin temperatures are relatively high, compared to experimentally achievable gate operation times [27].

Fig. 3(b) shows the pure dephasing rates as a function of the coupling parameter t. This parameter, which is also crucial for unitary operations on the two-qubit system, affects the dephasing rate via the energy difference between the singlet states, $\hbar\omega_0$, and via the mixing parameter ξ, which enters the spectral density. Obviously, the dephasing vanishes for uncoupled dots. However, for non-zero coupling, the dephasing rate grows rapidly with t. One can see that the dephasing rate increases as the distance between the dots D grows, which is a general feature of scattering-induced dephasing [24, 23].

Hyperfine interaction. The primary source of decoherence for a single electron spin confined in a QD is the hyperfine interaction between the electron spin and the spins of the nuclei of the surrounding atoms for many materials (see Refs [28, 29, 30] for review). The condition for the relevance of the hyperfine coupling is that at least some of the atoms have non-zero nuclear spin, which is usually the case (and example of a spinless material is especially purified silicon).

This interaction leads to pure dephasing at moderately high magnetic fields, but at lower magnetic fields a more involved decoherence process is observed which leads to a redistribution of the electron spin occupations. At low and intermediate magnetic fields the calculation of the evolution of the density matrix of the electron spin becomes difficult, because of the so called "flip-flop" terms in the hyperfine-interaction Hamiltonian. These terms cannot be treated perturbatively at low magnetic field values (the interaction can be regarded as a small perturbation with respect to the electron Zeeman splitting only at moderately high magnetic fields [30, 29]). Furthermore, the dependence of the hyperfine coupling constants on the location of a given nucleus with respect to the electron wave function substantially complicates the problem. This combined with the discrete structure of the nuclear spin environment [31] makes the problem strongly involved numerically.

A substantial simplification of the problem is obtained when the initial state of the nuclear

environment is limited to the infinite-temperature thermalized state. The assumption is not unreasonable, since the bath tends to relax quickly to a high-temperature state at experimentally accessible temperatures [31]. In this case, the "box model" can be used (also known as the uniform coupling model) for the whole range of magnetic field values [32, 33]. This is because the hyperfine-interaction-induced entanglement decay takes place on time scales much shorter than the "box model" limit of applicability, $t < N/A$, where N denotes the number of nuclei, and $A = \sum_k A_k$ is the sum of coupling constants between the electron and the nuclei.

The system under study can be described by the Hamiltonian (the magnetic field is applied in the z direction),

$$H = -g\mu_B \hat{S}^z B + \sum_k A_k \hat{S}^z \hat{I}_k^z + \frac{1}{2}\sum_k A_k \left(\hat{S}^+ \hat{I}_k^- + \hat{S}^- \hat{I}_k^+\right). \tag{13}$$

The first term in the Hamiltonian (13) is the electron Zeeman splitting, where g is the effective electron g-factor, μ_B is the Bohr magneton, $\hat{S}^z$ is the component of the electron spin parallel to the magnetic field, and B denotes the applied magnetic field. The last two terms describe the hyperfine interaction between the spin of an electron and the spins of the surrounding QD nuclei. The diagonal (second) term is also known as the Overhauser term and leads to pure dephasing, while the last term, known as the "flip-flop" term, is responsible for both dephasing and leveling out of the electron spin occupations. Here, $\hat{\mathbf{I}}_k$ are spin operators of the individual nuclei (discriminated by the index k). $\hat{I}_k^z$ is the component parallel to the applied magnetic field, while $\hat{I}_k^{\pm} = \hat{I}_k^x \pm i\hat{I}_k^y$ are the nuclear spin rising and lowering operators. Analogously, $\hat{S}^{\pm} = \hat{S}^x \pm i\hat{S}^y$ are the rising and lowering operators for the electron spin. The coupling constants of the hyperfine interaction depend on the species of the nuclei and on its location with respect to the electron wave function,

$$A_k = A_k^0 v_0 |\Psi(\mathbf{r}_k)|^2, \tag{14}$$

where $A_k^0 = \frac{2}{3}\mu_0 \gamma_e \gamma_k$ are the coupling strength constants of a given nuclear species found at site k, with μ_0 denoting the vacuum magnetic permeability, γ_e and γ_k being the electron and nuclear gyromagnetic ratios, respectively, while v_0 is the unit cell volume of the QD crystal, $\Psi(\mathbf{r})$ is the wave function of the electron located in the dot, and $\mathbf{r}_k$ is the position of the k-th nucleus.

The nuclear Zeeman term and the dipolar interaction between nuclei are omitted in the Hamiltonian (13). The first one was ignored because nuclear Zeeman energies of gallium and arsenic are very small, and the resulting energy splittings are of the order of tens of neV (corresponding to less than a mK) for each Tesla of magnetic field applied to the system. The nearest neighbor dipolar coupling constants between nuclei are even smaller, and are of the order of 0.1 neV. Hence, at typical experimental temperatures both nuclear terms in the Hamiltonian are much smaller than $k_B T$ and can be omitted [32, 30]. For the same reason the nuclear baths can be described by the infinite-temperature, fully mixed density matrices [31, 30] unless the state of the nuclear environment is especially experimentally prepared.

In the high-magnetic-field limit, $g\mu_B B > A$, for which the "flip-flop" term in the Hamiltonian (13) may be completely neglected, the Hamiltonian is diagonal and it is possible to find the QD state evolution for a realistic distribution of coupling constants A_k given by Eq. (14) while taking into account the large number of nuclei $N \sim 10^5$. The resulting dynamics is limited to pure dephasing which is further independent of the magnetic field (and local unitary oscillations that are irrelevant for the study of entanglement) for the initial high-temperature density matrix of the nuclear bath. The decay of a single spin is Gaussian and proportional to $\exp(-t^2/T_2^{*2})$ [32], with a characteristic time constant $T_2^* \approx \sqrt{\frac{6}{I(I+1)}}\sqrt{N}/A$, where the same spin I for all nuclei is assumed.

To quantify the single dot evolution at lower magnetic fields, the "box model" can be used which is valid on short time scales and which at high magnetic fields converges with the

approach introduced in the last paragraph. The upper limit of short-time-scale behavior is approximated by N/A [34]. In the "box model", the hyperfine coupling terms are assumed constant $A_k = \alpha = A/N$, which allows for the exact diagonalization of the Hamiltonian (13).

4.3.5 Quantum correlations [H2, H3, H5, H6]

Entanglement. Entanglement [35, 36] is one of the fundamental constituents of quantum theory. Correlations between the results of appropriately chosen measurements on entangled subsystems cannot be accounted for by any classical (realistic and local) theory [37], precluding the existence of a wide class of hypothetical more fundamental structures underlying the incompleteness of quantum description. Apart from its essential role in our understanding of the quantum world, entanglement is an important resource in quantum information processing [38] where it provides a quantum channel for teleportation [39], superdense coding [40], and distribution of cryptographic keys [41].

In order to manifest genuinely quantum behavior resulting from entanglement a quantum system must maintain phase relations between the components of its quantum superposition state, involving different states of distinct subsystems. Keeping in mind that the subsystems may be separated by a macroscopic distance, one may expect such a non-local superposition state to be extremely fragile to the dephasing effect of the environment. In fact, it has been shown (for a 2×2 system) that entanglement between two subsystems tends to decay faster than local coherence [42, 43, 44]. As expected, the decay of entanglement is stronger if the subsystems interact with different environments (which might result from a large spatial separation between them): certain states that show robust entanglement under collective dephasing become disentangled by separate environments [43]. Quite remarkably, it was shown for two different classes of systems [44, 45] that certain states may become separable (completely disentangled) within a final time under conditions that lead to usual, exponential decay of local coherence. Since even partial entanglement of many copies of a bipartite quantum system may be still distilled to a smaller number of maximally entangled systems [46], it seems essential to understand whether environmental influence leads to appearance of separability in realistic models of dephasing.

For a quantitative description of the decay of entanglement, a measure of entanglement that may be calculated from the system state is needed. For pure states, von Neumann entropy of one subsystem [47] may be used but for mixed states there is no unique entanglement measure [48, 49]. One choice is to use the *entanglement of formation* (EOF), defined as the ensemble average of the von Neumann entropy minimized over all ensemble preparations of the state [49]. Such a measure may be interpreted as the asymptotic number of pure singlets necessary to prepare the state by local operations and classical communication. A practical characterization for mixed state entanglement is available for small systems [50, 51] but an explicit formula for calculating an entanglement measure is known only for a pair of two-level systems [52, 53].

The two-qubit EOF can be calculated from their density matrix $\rho(t)$ using the formula [52, 53]

$$E[\rho(t)] = E[\rho(t)] = -x_+ \log_2 x_+ - x_- \log_2 x_-, \tag{15}$$

where $x_\pm = (1 \pm \sqrt{1 - C^2[\rho(t)]})/2$, and $C[\rho(t)]$ is called the Concurrence, given by

$$C[\rho(t)] = \max(0, \lambda_0 - \lambda_1 - \lambda_2 - \lambda_3), \tag{16}$$

where λ_i are the square roots of the eigenvalues of the matrix $\rho(t)(\sigma_y \otimes \sigma_y)\rho^*(t)(\sigma_y \otimes \sigma_y)$ in decreasing order. $\rho^*(t)$ denotes the complex conjugate of the density matrix $\rho(t)$. Note that the Concurrence is also an entanglement measure. It is commonly used to quantify two-qubit entanglement because of the mathematical simplicity with which it is calculated.

Entanglement decay of a two excitonic qubits [D3] Two excitonic qubits interacting with a phonon baht are described by the Hamiltonian (6). The two-qubit evolution can be

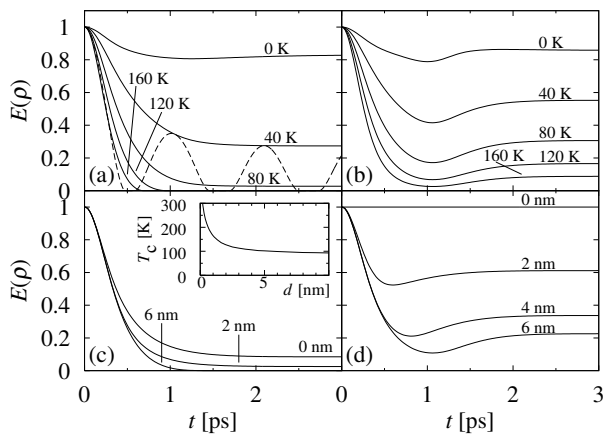

Figure 4: Evolution of entanglement of the two-qubit system at various temperatures with $d = 6$ nm (a,b) and for various distances d at $T = 100$ K (c,d). The left panels (a,c) show the result for the initial state (17a) and the right ones (b,d) for the singlet state (17b). The inset in (c) shows the lowest temperature at which the decay becomes complete for a given distance. Solid lines correspond to $\Delta E = 0$ and the dashed line to $\Delta E/\hbar = 6$ ps^{-1} (at $T = 40$ K).

found using the Weyl operator method (3). Once the evolution is found, the decay of entanglement can be calculated using the Concurrence 16) or the EOF (15).

The evolution of the EOF of the qubit pair initially in one of the two maximally entangled states

$$|\psi_0\rangle = \frac{1}{2}(|00\rangle + |01\rangle + |10\rangle - |11\rangle), \tag{17a}$$

$$|\psi_B\rangle = \frac{1}{\sqrt{2}}(|01\rangle - |10\rangle). \tag{17b}$$

is shown in Fig. 4. In the absence of energy shift ΔE (solid lines), entanglement decays on a time scale of a few picoseconds. At low temperatures or for overlapping systems, this process resembles the decay of coherences in a single system under the same environmental influence [54]. However, for a sufficiently large separation between the systems and at sufficiently high temperatures the initially maximal entanglement present in the state (17a) decays completely after a finite time even though the environment-induced dephasing is always only partial (see Fig. 4a,c). The temperature T_c at which the systems get completely disentangled is related to the distance as shown in the inset in Fig. 4c. On the other hand, for the other initial state [Eq. (17b)], the destruction of entanglement is always only partial (Fig. 4 b,d).

An important case is that of $\Delta E \neq 0$. Such an energy shift (known as biexcitonic shift in semiconductor system) leads to an entanglement-generating evolution. This mechanism is used for performing nontrivial two-qubit gates (controlled-shift) in many proposals for semiconductor-based quantum information processing [55, 56]. As can be seen in Fig. 4 (dashed line), in the presence of phonon-induced pure dephasing the cyclic evolution of entanglement is damped and the maximum achievable level of entanglement is reduced. Moreover, extended periods of time appear when the entanglement remains zero.

The appearance of complete disentanglement for some initial states under sufficiently strong partial pure dephasing may be understood with the help of Eq. (16). If the completely dephased state (with a diagonal density matrix) has $\lambda_0 - \lambda_1 - \lambda_2 - \lambda_3 < 0$ then, by continuity, it will be surrounded by states with vanishing concurrence so that entanglement vanishes for sufficiently strongly dephased states, before the complete dephasing is reached. Form the Wootters formula for a diagonal density matrix one finds $\lambda_0 - \lambda_1 - \lambda_2 - \lambda_3 = -2\min(\rho_{00}\rho_{33}, \rho_{11}\rho_{22})$, so that the above condition may only be satisfied if all four diagonal elements are nonzero, which is the case for the initial state (17a) but not (17b).

The decay of effective entanglement of two excitonic qubits [H2]. In earlier analysis of entanglement evolution, it was assumed that the observer has the power to perform arbitrary measurements and can determine the state of the system completely. This is however not always true. In particular, there are natural systems, like QDs, where limited measurement power is a natural and practical constraint (ie. single electron transistors (SETs) coupled to QD systems can be used to find a limited amount of information about the QD state [57, 58]). In all such

cases of limited measurement capability, it is natural to consider the worst case scenario: as real entanglement, one should consider the entanglement (i.e. chosen entanglement measure) minimized over the set of measurement data. The minimized entanglement will subsequently be called effective entanglement.

Here, the system is identical to the one considered in the previous paragraph. The limitations to the knowledge of the system state imposed by a realistic measurement setup (consisting of different configurations of SETs interacting with the double-dot system) are taken into account. This measurement scheme does not allow for state tomography and provides, in fact, a very limited set of observables. In each time-step we minimize the value of entanglement with respect to the data which can be measured and find the evolution of the effective entanglement with respect to the SET-defined observables, for the sake of clarity. The set of attainable observables is given by

$$x = \langle 00|\rho|00\rangle + \langle 01|\rho|01\rangle, \tag{18a}$$
$$y = \langle 00|\rho|00\rangle + \langle 10|\rho|10\rangle, \tag{18b}$$
$$z = \langle 01|\rho|01\rangle + \langle 10|\rho|10\rangle + 2\mathrm{Re}\langle 01|\rho|10\rangle, \tag{18c}$$
$$d = \langle 11|\rho|11\rangle; \tag{18d}$$

the physical justification for such a choice is given in Ref. [H2].

Firstly, the situation is considered, when a number of SETs provide all possible information that can be gained about the state of the double QD with this measurement technique. Since all of the diagonal density matrix elements are known, the set of initial maximally entangled states which cannot exhibit sudden death of effective entanglement is the same as the set of states with real off-diagonal density matrix elements which do not exhibit sudden death of physical entanglement [D3]. The time evolution of effective and physical entanglement in these states under pure dephasing is the same. The situation is different for states where all diagonal density matrix elements are non-zero where the set of effectively entangled coherent states is substantially reduced.

Secondly, the situation is considered when only x and z have been measured, so only linear combinations of some density matrix elements are known. The measurement outcome $x \in [0, 1]$. The outcome $z \in [0, 2]$, but it is easy to show that for non-zero effective entanglement $z > 1$. It is interesting to consider here the time-evolution of effective entanglement under phonon-induced pure dephasing of an initially maximally entangled state $|+\rangle$, with $|\pm\rangle = (|01\rangle \pm |10\rangle)/\sqrt{2}$. When measured it will yield $x = 0.5$ and $z = 2$, so the effective concurrence $C_e(|+\rangle\langle +|) = 1$ (note that the state $|-\rangle$ has $x = 0.5$, but $z = 0$ and $C_e(|-\rangle\langle -|) = 0$). Phonon-induced evolution of the state does not change x, but z decreases with decreasing $\mathrm{Re}(h)$ leading to sudden death of effective entanglement for sufficiently dephased states. This state does not exhibit sudden death of physical entanglement.

Thirdly, the simplest situation is considered, where the measurement data yield only z as defined in Eq. (18c). The amount of information gained by the measurement is very limited. The dependence of effective entanglement on z is plotted in the inset of Fig. 5. The evolution of effective entanglement of the initial state $|+\rangle$ in this setup under realistic phonon-induced pure dephasing is plotted in Fig. 5 for different temperatures. As is to be expected, effective disentanglement occurs faster than physical disentanglement. Furthermore, sudden death of entanglement appears for sufficiently high temperatures (e. g., when the dephasing is strong enough). For a limited range of temperatures, sudden birth of entanglement is also observed. The second phenomenon is due to the enhancement of coherence which occurs when wavepackets from the two QDs meet due to positive interference between them; this mechanism does not lead to the sudden birth of physical entanglement [D3].

Entanglement decay of QD spin qubits [H5]. In the following, the evolution of entanglement of two non-interacting electron spin qubits confined in two well separated self-assembled

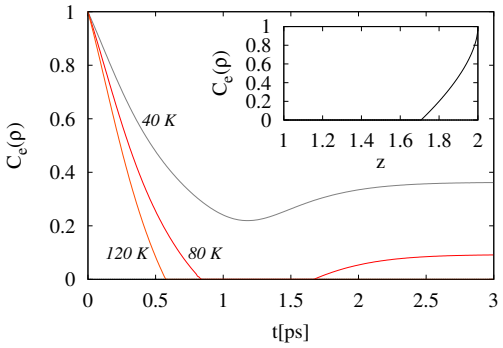

Figure 5: The time-evolution of effective entanglement for different temperatures. Inset: Effective entanglement as a function of the measured parameter z

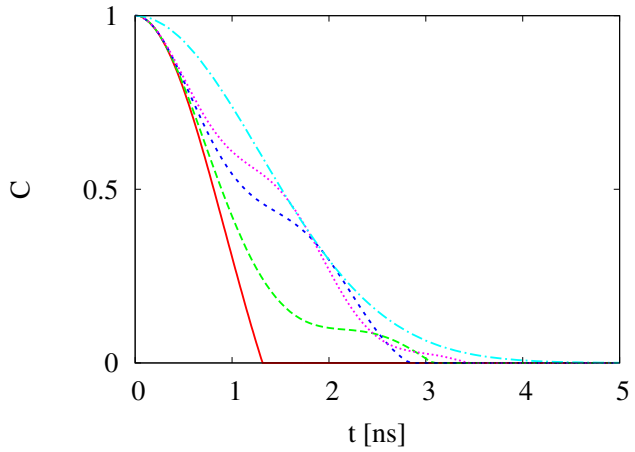

Figure 6: Time evolution of entanglement for different magnetic field values, $B = 0$ - solid red line, $B = 11$ mT - long dashed green line, $B = 16.5$ mT - dashed blue line, $B = 20$ mT - dotted pink line, and $B = 1$ T - dashed/dotted blue line (high magnetic field limit).

GaAs QDs is studied. The qubits interact with separate nuclear spin reservoirs via the hyperfine coupling, which are both taken in the high-temperature thermalized state. The setup is described by the Hamiltonian (13) and the method of finding the evolution of the state of the QDs is outlined in a previous section.

The study is restricted to initial Bell states,

$$|\Psi^{\pm}\rangle = 1/\sqrt{2}(|1\rangle \pm |2\rangle), \tag{19a}$$
$$|\Phi^{\pm}\rangle = 1/\sqrt{2}(|0\rangle \pm |3\rangle), \tag{19b}$$

where the states in the single QD basis are equal to $|0\rangle = |\uparrow\uparrow\rangle$, $|1\rangle = |\uparrow\downarrow\rangle$, $|2\rangle = |\downarrow\uparrow\rangle$, and $|3\rangle = |\downarrow\downarrow\rangle$. The evolution of the coherences for these initial states is limited to the single off-diagonal element of the density matrix which is initially non-zero, while the other coherences remain zero at all times. Contrarily, all four occupations are influenced (except for the high-magnetic-field limit where the decoherence is a pure dephasing process) by the interaction. Hence, the double QD density matrix is simplified and the concurrence is always of the form,

$$C(\rho_{DQD}) = 2\max\{0, |\rho_{ij}| - \sqrt{\rho_{kk}\rho_{ll}}\}, \tag{20}$$

where i, j are equal to $1, 2$ or $0, 3$ depending on the initial state, and $k \neq l$, $k \neq i$, $k \neq j$, $l \neq i$, $l \neq j$. It is evident from Eq. (20) that sudden death of entanglement will occur when $|\rho_{ij}| < \sqrt{\rho_{kk}\rho_{ll}}$, so sudden death is expected in the low magnetic field regime when the QD occupations are disturbed, while it will not occur for high magnetic field pure dephasing. Furthermore, because the qubits interact with separate environments at high temperature thermal equilibrium, the evolution of entanglement is the same for all four initial Bell states.

Fig. 6 shows entanglement decay for different magnetic field values. The zero magnetic field curve (red solid) limits all higher magnetic field curves from below and ends in SD. The high magnetic field curve (dashed/dotted blue line), provides the upper limit for the concurrence at a given time and undergoes exponential decay. In between, the curves corresponding to small magnetic fields display a more complex entanglement evolution. According to Eq. (20),

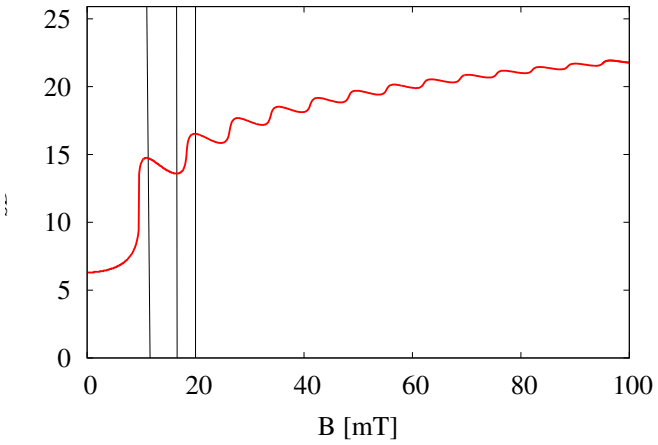

Figure 7: Entanglement SD time t_{SD} as a function of the magnetic field. The vertical lines mark the magnetic field values corresponding to the long dashed green, dashed blue and dotted pink lines in Fig. 6. Between 5 and 10 mT the SD time is a good indicator of the magnetic field value.

the visible oscillations are due to the interplay of the dephasing process and the shifts in the occupations. The number of oscillations increases with the increase of the magnetic field, while they become less pronounced, because the high magnetic field inhibits occupation changes. The suppression of the oscillations is a manifestation of the transition between the two types of disentanglement.

It is due to those oscillations that the SD times are not a monotonous function of the magnetic field, as seen in Fig. 7. At low magnetic fields, a strong oscillatory behavior is evident, starting from around 10 mT. For higher magnetic fields, ρ_{ij} decays as $\exp[-\sigma^2 t^2]$, while $\rho_{kk} = \rho_{ll}$, which initially equals 0, oscillates with the amplitude proportional to $\frac{\sigma^2}{B^2}$, where $\sigma^2 \sim A^2/N$. The equality between the two, responsible for SD of entanglement, gives an estimated $t_{SD} \sim \sqrt{2 \ln \frac{B}{\sigma}}/\sigma$ valid for high magnetic fields.

The quantity $W(t) = F - \frac{1}{2} = \langle \Psi_- | \rho(t) | \Psi_- \rangle - \frac{1}{2}$ (which is an entanglement witness) allows the identification of the exact time sudden death of entanglement occurs, which corresponds to $W(t) = 0$. This means that the zero point t^* of $W(t)$ ($W(t^*) = 0$) is just a sudden death time ($t^* = t_{SD}$ and as such has exactly the same dependence on the magnetic field as shown in the Fig. 7). Quite remarkably, W as an entanglement witness is directly measurable. Thus by measuring this quantity we may get the exact estimate of the magnetic field whenever it corresponds to the initial monotonic regime of the function. In the regions close to the steep parts of the function the above value is quite sensitive to the field B and can be considered as a threshold sensor of the latter. Thus by measuring this quantity we may get the estimate of the magnetic field. In the regions close to the steep parts of the function the above value is quite sensitive to the field B and can be considered as a threshold sensor of the latter in the regime between 5 mT and 10 mT for the QD parameters considered.

Quantum discord. The quantum discord [59, 60], a measure of bi- and multi-partite quantum correlations, has attracted much attention recently. This is due to the fact that the discord indicates the existence of quantum correlations in many partially mixed states which have no entanglement present. Specifically, the quantum discord does not display any sudden death type phenomenon, since the set of zero-discord states has no volume [61]. Hence, a smooth, continous decoherence process, such as pure dephasing cannot lead to a sudden and continued dissapearance of quantum correlations mid-evolution (before a fully mixed, completely dephased state is reached). This suggests that the sudden death of entanglement signifies not, as was previously believed, the dissapearance of all quantum correlations, but the crossing of a threshold of a given, small amount of correlations. Although beneath this threshold many quantum informational tasks may no longer be performed, methods of performing quantum computation on zero-entanglement states for which the quantum discord is non-zero have already been devised [62, 63, 64]. Furthermore, it has been very recently shown experimentally

how entanglement can be shared between distant parties via non-entangled states with non-zero discord [65].

The quantum discord is defined as the difference between two classically equivalent formulas for mutual information [59]. The formula which is referred to as mutual information in Ref. [66] is given by [59]

$$\mathcal{I}(\rho_{AB}) = S(\mathrm{Tr}_A\,\rho_{AB}) + S(\mathrm{Tr}_B\,\rho_{AB}) - S(\rho_{AB}), \tag{21}$$

where the von Neumann entropy is given by $S(\rho) = -\mathrm{Tr}\,\rho\log_2\rho$. This quantity has been generalized from the classical language of probability distributions in a straightforward manner to the language of dencity matrices, while the Shannon entropy was replaced by von Neumann entropy. The other formula for classical mutual information, which is in the quantum context referred to as classical correlations (in Ref. [66]), cannot be generalized in a direct manner, because the classical formula involves conditional entropy,

$$\mathcal{C}(A:B) = H(A) - H(A|B),$$

where H denotes the Shannon entropy and A and B are random variables. Conditional entropy $H(A|B)$ requires the specification of the state of A given the state of B, which in quantum mechanics is ambigous until the measurement performed on B is specified. Hence, the conditional von Neumann entropy can be found given the complete measurement on subsystem B and the resulting formula for classical correlations is [59, 60]

$$\mathcal{C}(\rho_{AB}) = \max_{\{\Pi_k\}}\left[S(\mathrm{Tr}\,\rho_{AB}) - S(\rho_{AB}|\{\Pi_k\})\right], \tag{22}$$

where $\{\Pi_k\}$ is a complete set of orthonormal projective operators corresponding to a von Neumann measurement of subsystem B. The index k denotes the outcome of a given measurement and the formula involves maximization over the set of projective measurements. Therefore the formula of Eq. (22) yields the information gained about the system A after the measurement $\{\Pi_k\}$ on system B. The quantum discord of a given state ρ_{AB} is then given by

$$D(\rho_{AB}) = \mathcal{I}(\rho_{AB}) - \mathcal{C}(\rho_{AB}). \tag{23}$$

Unfortunately, computing the quantum discord for an arbitraty density matrix is an extrememely involved task even in the simplest two-qubit case. This led to the emergence of the geometric quantum discord [67], which is defined as the minimal Hilbert-Schmidt distance of a given state from the set of zero-discord states. Although an explicit formula for the geometric discord given a two-qubit density matrix does not yet exist (one that does not require minimization over the set of all zero-discord states), such formulas exist for the lower [67] and upper [68] bounds on the geometric discord.

The lower bound on the discord is given by [67]

$$D'_S = \max\left(\mathrm{Tr}[K_x] - k_x, \mathrm{Tr}[K_y] - k_y\right), \tag{24}$$

where k_x is the maximum eigenvalue of the matrix $K_x = |x\rangle\langle x| + TT^T$ and k_y is the maximum eigenvalue of the matrix $K_y = |y\rangle\langle y| + T^TT$. Here, $|x\rangle$ and $|y\rangle$ denote local Bloch vectors with components $x_i = \mathrm{Tr}[\rho_{AB}(\sigma_i\otimes\mathbb{I})]$ and $y_i = \mathrm{Tr}[\rho_{AB}(\mathbb{I}\otimes\sigma_i)]$, and the elements of the correlation matrix T are given by $T_{i,j} = \mathrm{Tr}[\rho_{AB}(\sigma_i\otimes\sigma_j)]$ (stemming from the standard Bloch representation of a two-qubit density matrix ρ_{AB}). The upper bound is given by [68]

$$D''_S = \min\left(\mathrm{Tr}[K_x] - k_x + \mathrm{Tr}[L_y] - l_y\,\mathrm{Tr}[K_y] - k_y + \mathrm{Tr}[L_x] - l_x\right), \tag{25}$$

where l_x and l_y are the maximal eigenvalues of the matrices $L_x = |x\rangle\langle x| + T|\hat{k}_y\rangle\langle\hat{k}_y|T^T$ and $L_y = |y\rangle\langle y| + T^T|\hat{k}_x\rangle\langle\hat{k}_x|T$, respectively, while $|\hat{k}_x\rangle$ and $|\hat{k}_y\rangle$ are the normalized eigenvectors corresponding to the eigenvalue k_x of matrix K_x and k_y of matrix K_y. In the case of symmetric

two-qubit states, meaning $\rho_{AB} = \rho_{BA}$, no minimization or maximization is needed in eqs. (24) and (25).

The upper and lower bounds often coincide, yielding the true value of the geometric discord. This is specifically the case for pure states, Bell diagonal states, and states with vanishing local Bloch vectors, $|x\rangle = |y\rangle = 0$ [68]. Hence, it is straightforward to show that the geometric discord is equal to 1/2 for all maximally entangled two-qubit states [69],

$$|\psi\rangle = 1/\sqrt{2}(a|00\rangle + \sqrt{1-a^2}e^{i\alpha}|10\rangle + \sqrt{1-a^2}e^{i\beta}|01\rangle - ae^{i(\alpha+\beta)}|11\rangle). \tag{26}$$

Here $a \in [0, 1]$, while α and β are arbitrary.

The geometric discord is a good measure to distinguish between zero-discord and non-zero-discord states, but because of the properties of the Hilbert-Schmidt distance, it is not a good measure for the amount of quantum correlations present in a given state. In fact, because the Hilbert-Schmidt distance is sensitive to the purity of the state, the geometric discord may be increased by non-unitary evolution of a single qubit (the unmeasured one) [70, 71], which should not increase inter-qubit quantum correlations.

One solution of this problem has been proposed in Ref. [72]. It turns out that to diminish the sensitivity of the Hilbert-Schmidt distance to the purity of the states, it suffices to normalize each state by its Hilbert-Schmidt norm, namely to define a distance between two states ρ_1 and ρ_2 as

$$d_T(\rho_1, \rho_2) = \left|\left| \frac{\rho_1}{||\rho_1||} - \frac{\rho_2}{||\rho_2||} \right|\right|, \tag{27}$$

where $||\cdot||$ is the Hilbert-Schmidt norm. The rescaled discord is then defined as the distance between a given state and the nearest zero-discord state, using the distance measure (27) and for a two-qubit state it is found to be

$$D(\rho) = \frac{1}{2}\left(1 - \frac{\sqrt{3}}{2}\right)\left[1 - \sqrt{1 - \frac{D_S(\rho)}{2\,\mathrm{Tr}\,\rho^2}}\right]. \tag{28}$$

Here, $D_S(\rho)$ denotes the geometric discord and $\mathrm{Tr}\,\rho^2$ is the purity of the studied state.

The evolution of the quantum discord of excitonic qubits [H3]. Here, we study the evolution of the lower and upper bounds of the geometric discord [see Eqs (24) and (25)] of two excitonic qubits interacting with an open phonon environment in order to capture the physical aspects of decoherence effects on quantum correlations. The specific system under study is described by the Hamiltonian (6) and the evolution is obtained as described before.

As it turns out, the geometric discord for initial Bell states under any pure dephasing process is equal to $D_S(t) = 2|\rho_{ij}(t)|^2$ since they retain their Bell-diagonal form throughout the evolution. Here, ρ_{ij} denotes the off-diagonal element of the two-qubit density matrix which is non-zero. Note that up to a normalization factor, the value of the geometric discord in this case yields the square of the Concurrence.

Let us first study the evolution of the mixed X-state,

$$\rho = \begin{pmatrix} a & 0 & 0 & ag_{03}(t) \\ 0 & b & bg_{12}(t) & 0 \\ 0 & bg_{12}^*(t) & b & 0 \\ ag_{03}^*(t) & 0 & 0 & a \end{pmatrix}, \tag{29}$$

which is significantly simpler, but already carries some of the properties of the discord evolution of a pure initial state with all coherences present. The entanglement of such a state, measured by the concurrence, is equal to $C(t) = \max\{0, b|g_{12}(t)| - a, a|g_{03}(t)| - b\}$ and is prone to sudden death. The geometric discord is given by

$$D_S(t) = \begin{cases} (a|g_{03}(t)| - b|g_{12}(t)|)^2 + (a-b)^2, & \text{for } |a-b| < a|g_{03}(t)| + b|g_{12}(t)| \\ 2a^2|g_{03}(t)|^2 + 2b^2|g_{12}(t)|^2, & \text{for } |a-b| > a|g_{03}(t)| + b|g_{12}(t)|. \end{cases} \tag{30}$$

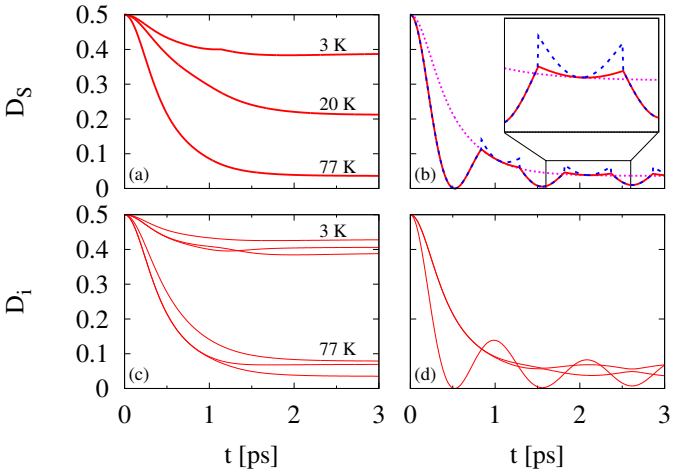

Figure 8: Evolution of geometric discord bounds at $d = 6$ nm for pure initial state (26) with $a = 1/\sqrt{2}$ (a,b) at different temperatures for $\Delta E = 0$ for which the upper and lower bounds are equal (a) and at 77 K for $\Delta E = 6$ ps^{-1}; red solid line - lower bound, blue dashed - upper bound, pink dotted - $\Delta E = 0$ (b). Lower bound values corresponding to the three eigenvalues of the matrix K_x (the minimum of which yields the geometric discord lower bound) at different temperatures for zero biexcitonic shift (c) and and at 77 K for $\Delta E = 6$ ps^{-1} (d).

Hence, the discord will not undergo sudden-death-like behavior, but, if $a \neq b$, it will display a transition between two types of decay (there is no simple relation between the transition point and the point of entanglement sudden death). The transition point coincides with the transition point between quantum and classical decoherence indicated in Ref. [66].

The next step is to study the evolution of the lower and upper geometric discord bounds for an initial state (26) with all non-zero coherences ($a \neq 0$ and $a \neq 1$) under phonon-induced partial pure dephasing. For simplicity the studied state is taken with $a = 1/\sqrt{2}$ (the local phases α and β do not change the values of the geometric discord or either of its bounds). On Fig. 8 (a) the evolutions of the geometric discord are plotted at different temperatures for zero biexcitonic shift (the upper and lower bounds are equal in this case). The 3 K curve shows a distinct point where the discord is not smooth, resembling the evolution of the X-state (29), which is absent at higher temperatures. To understand this, the evolutions of $D_i = \mathrm{Tr}[K_x] - k_i$, where k_i are the three eigenvalues of the matrix K_x (the minimum of D_i yields the true lower bound of the geometric discord) for 3 and 77 K are plotted in Fig. 8 (c). At 3 K a crossing of two D_i curves is observed which is caused by the positive interference of phonon wave packets, which is responsible for the enhancement of the geometric discord for the X-state of eq. (29).

Fig. 8 (b) shows the evolution of the lower (red solid line) and upper (blue dashed line) bounds on the geometric discord for the same initial state at 77 K when the biexcitonic shift is nonzero. The biexcitonic shift in the absence of any decoherence processes causes a coherent oscillation between the initial, maximally entangled state, and the separable state $|\psi_{\mathrm{sep}}\rangle = 1/2(|0\rangle + |1\rangle) \otimes (|0\rangle + |1\rangle)$ (reached when $\Delta E t = (2n+1)\pi$, where n is a natural number). Under phonon-induced pure dephasing, the oscillations of entanglement are damped and display prolonged periods when the entanglement is zero (which is only possible when the damping process can lead to sudden death of entanglement), and are otherwise smooth while their amplitude is limited by the entanglement decay displayed by the zero-biexcitonic shift evolution [D3]. The oscillations of the geometric discord, which without decoherence would mimic entanglement oscillations, are substantially different. Firstly, the discord does not display sudden-death-type behavior. Furthermore, the evolution of the quantum discord induced by the biexcitonic shift leads to the situation, when the value of the geometric discord is greater than the corresponding zero-biexcitonic-shift value. This shows that the dependence of the discord on quantum phase relations is non-trivial, and than non-local phase correlations may lead to an enhancement of quantum correlations in mixed states depending on the actual value of the phase factor.

Although the studied quantity here was the geometric discord, note, that rescaling all of the presented results using Eq. (28), which would yield the rescaled geometric discord which is

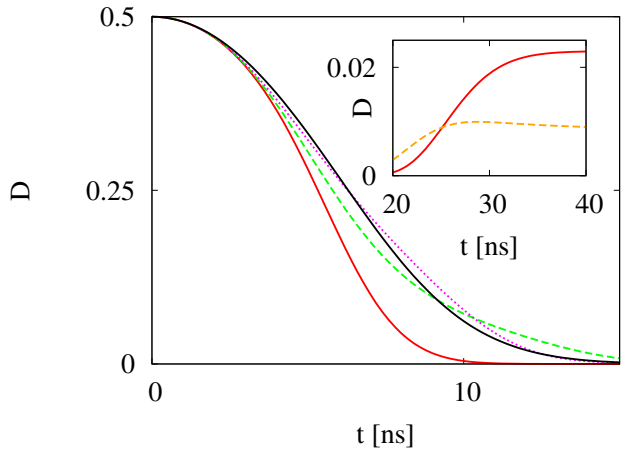

Figure 9: Time-evolution of the rescaled discord of the initial Bell state for different magnetic fields: B=0 (solid red line; lower bound on the plots), B=11 mT (dashed green line), B=16.5 mT (dotted magenta line), B= 1T (blue dashed-dotted line). The inset shows long-time evolution, revealing partial revival of the discord for small magnetic fields: B=0 (solid red line) and B=3 mT (orange dashed line).

insensitive to the purity of the studied two-qubit state, would not change any of the qualitative behaviour of the discord evolution which is presented above.

The evolution of the quantum discord of QD spin qubits [H6]. Let us return to the of two electron spins confined in two, well separated lateral QDs interacting with a nuclear bath as descibed by the Hamiltonian (13). Bell states (19) are natural fully entangled states to be studied in a double spin-in-a-QD system (as in many other realistic scenarios), since they are initialized more easily than other entangled states. Their evolution is always Bell diagonal, hence the density matrix of the two-qubit system is of the form

$$\rho_{DQD}(t) = \begin{pmatrix} \frac{1}{2} - a(t) & 0 & 0 & 0 \\ 0 & a(t) & b(t) & 0 \\ 0 & b^*(t) & a(t) & 0 \\ 0 & 0 & 0 & \frac{1}{2} - a(t) \end{pmatrix}. \tag{31}$$

The initial conditions for any Bell state are $a(t) = 1/2$ and $b(t) = \pm 1/2$, with the basis states in the density matrix (31) arranged in the order $|0\rangle$, $|1\rangle$, $|2\rangle$, $|3\rangle$ for initial states (19a) and in the order $|1\rangle$, $|0\rangle$, $|3\rangle$, $|2\rangle$ for initial states (19b).

Since the lower and upper bounds on the rescaled discord D coincide for any Bell diagonal state, they coincide throughout the hyperfine-interaction induced evolution of any initial Bell state. Furthermore, analytical formulas for the values of D_S can be found in a straightforward manner for this type of evolution, which can then be extended using Eq. (28) to yield the value of D. Indeed the formula for the geometric quantum discord reads

$$D_S(\rho_{DQD}(t)) = \begin{cases} 2|b(t)|^2 \text{ for } g(t) \leq 1, \\ \left[\frac{1}{2} - 2a(t)\right]^2 + |b(t)|^2 \text{ for } g(t) \geq 1, \end{cases} \tag{32}$$

where

$$g(t) = \frac{2|b(t)|}{|1 - 4a(t)|}. \tag{33}$$

The purity necessary to find the rescaled discord is equal to

$$P(\rho_{DQD}(t)) = 2\left[(\frac{1}{2} - a(t))^2 + a^2(t)\right] + 2|b(t)|^2. \tag{34}$$

Note, that rescaling D_S, although it affects the curves of the time-evolution, does not change the transition point between the two regimes of the discord decay.

Fig. (9) shows the time-evolution of any initial Bell state for different magnetic field values. Contrarily to the time-evolution of entanglement of the same system [H5], oscillations of the rescaled discord D are hardly visible. Furthermore, although the values of D are limited from

below by the zero-magnetic-field curve as in the case of entanglement, they are not limited from above by the infinite-magnetic-field line (contrarily to entanglement). This is due to the shape of the decay of the amplitude of the single coherence present, $|b(t)|$, which is weakly enhanced or slowed by the oscillations of the QD occupations. At long time scales, which are shown in the inset of Fig. (9), a small revival of the discord is observed at very low magnetic fields (seen for $B = 0$ T and $B = 3$ mT), which originates from the small revival of the coherence characteristic of low magnetic fields and the zero-volume quality of the zero-discord states which makes discord revivals very common.

It turns out that regardless of the magnetic field, the decay of the discord for initial Bell states is always confined to the $g(t) \leq 1$ limit, where the value of the geometric discord is proportional only to the square of the amplitude of the coherence (which is then rescaled according to Eq. (28) to get the rescaled discord).This is explained in terms of energy conservation in [H6].

For zero-magnetic-field, although the coherence experiences an involved evolution pattern, including a revival after the initial strong decay is complete, the coherence and the occupations always satisfy the relation $g(t) = 1$. For non-zero magnetic field, the dephasing is faster than the decay of occupations, thus $g(t) < 1$ for all times except $t = 0$.

Note that the behavior of the discord evolution for long times shows strong dependence on small magnetic fields in the range $0-5$ mT (see inset of Fig. 9). The ability to perform precise rescaled discord measurements would enable one to detect small magnetic fields. The proposed procedure would expand the region of applicability of a QD magnetic sensor to the region of magnetic fields inaccessible to the entanglement based procedure. Here, entanglement is not required as a necessary resource for these long-time measurements - the results can be obtained using X-states (29) with zero entanglement and non-zero discord.

The idea sketched above is not the only possibility of detecting small magnetic field values taking advantage of the rich characteristics of the decoherence driven discord evolution. Other possibilities are discussed extensively in Ref. [H6].

4.3.6 QPC measurement of double QD spin states and phonons [H4, H7]

QPC measurements of charge states. The quantum point contact (QPC) [73] measurement of charge states in a lateral double QD defined by gate potentials in a two dimensional electron gas involves monitoring the current flowing through the QPC which depends on the occupation of the QDs due to a Coulomb interaction between the electrons confined in the QD and electrons traveling through the QPC [74, 57]. This measurement scenario is a realization of the so called weak measurement [38], where the measured system is only weakly coupled to the measuring device. Contrary to the projective measurement, this measurement is not instantaneous, as both the localization of the QD states into the measurement basis and acquiring the data needed to distinguish between the basis states take time. Apart from the measurement time, another relevant factor is the attainable distinguishability of states, since even after an infinitely long measurement time it may not be possible to completely distinguish between the measurement basis states. On the other hand, a weak measurement is typically less destructive to the measured system than an instantaneous projective measurement. Furthermore, such a measurement is the only option in many involved quantum systems which are hard to access experimentally. Hence, the QD-QPC measurement setup is commonly used experimentally to study QD occupations at very low temperatures [75, 76, 77, 78, 79, 80, 6]. As we have previously shown, phonon effects do not interfere with the charge measurement in any significant way [E4], since while they strongly affect the coherence times of QD states, phonons do not affect the localization times or the distinguishability between the measurement basis states in this setup.

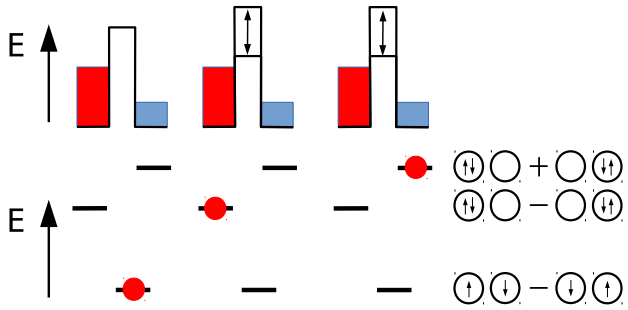

Figure 10: Schematic representation of the changes of the QPC barrier height due to Coulomb interaction with different spatial configurations of the three spatially distinct double QD spin singlet states. The top part shows the QPC barrier height corresponding to the occupation of the double QD represented in the bottom part of the figure. The two doubly occupied states are superpositions of configurations with charges adjacent or remote from the QPC which results in fluctuations of the QPC barrier.

QPC measurement of singlet-triplet spin qubits. The measurement of spin states of electrons confined in QDs is much more complicated and typically involves spin-to-charge conversion prior to a QPC measurement of the charge [76, 79, 6, 8]. An alternative scheme for the direct measurement of the spin symmetry (singlet-triplet) of two-electron states confined in a double QD was proposed in Ref. [74]. Here, the quality of the measurement relies on QPC current noise being different for the singlet and triplet spin symmetries. The disparity of current fluctuations is due to the fact that, according to Pauli exclusion principle, states with both electrons localized in the same QD are allowed in the spin-singlet configuration, but not for spin-triplet case. Hence, the electron charge distribution will fluctuate during the measurement process due to the QD-QPC interaction only if the electrons are in the spin-singlet state, leading to enhanced QPC current noise for this spin configuration.

The Hamiltonian of the double QD system with two electrons is given by Eq. (10). The eigenstates of this Hamiltonian are the three spin triplet states given by Eqs (11) and the three spin singlet states given by Eqs (12), which allow for double QD occupations.

The QPC is situated near one of the QDs in such a way that it is sensitive to the occupation of only this one (right) dot. The double QD-QPC interaction is described by the Hamiltonian

$$H_{\rm tun} = \sum_{p,q,\sigma} (T_{pq} + \chi_{pq} n_R) a^\dagger_{Sp\sigma} a_{Dq\sigma} + \text{H.c.}, \tag{35}$$

which accounts for the tunnelling of electrons through the QPC and contains a factor dependent on the occupation of the right dot, n_R. Hence, electron tunnelling consists of a robust part, independent of the QD occupation described by the constants T_{pq}, and a Coulomb interaction induced enhancement χ_{pq}. The tunnelling constants are assumed to be slowly varying over the energy range where tunnelling is allowed [82, 74] and are taken constant. Here, $a_{np\sigma}$, $a^\dagger_{np\sigma}$ are the QPC electron annihilation and creation operators corresponding to an electron in lead $n = \mathrm{S}, \mathrm{D}$ (source, drain) and in mode p, with the distinction of spin σ which is constant throughout the tunnelling. In this paper, we study a QPC which operates in the high bias regime, that is, in the situation when the chemical potential offset between the leads is large enough to induce transitions to doubly excited states [74].

The evolution of the double QD system is found using the Lindblad master equation,

$$\dot\rho(t) = \mathcal{L}(\rho) = -\frac{i}{\hbar}[H_{\rm DQD}, \rho] + \frac{1}{\hbar^2}\left(\sum_i^3 \frac{1}{2}(C_i^\dagger C_i \rho + \rho C_i^\dagger C_i) + \sum_i^3 C_i \rho C_i^\dagger\right) \tag{36}$$

where the Lindblad operators are given by [74]

$$C_1 = \nu\sqrt{\frac{V-\Delta}{\hbar}}\sin\frac{\theta}{2}|(-)S\rangle\langle S_-|, \tag{37a}$$

$$C_2 = \nu\sqrt{\frac{V+\Delta}{\hbar}}\sin\frac{\theta}{2}|S_-\rangle\langle(-)S|, \tag{37b}$$

$$C_3 = \sqrt{\frac{V}{\hbar}}\left[(\mathcal{T}+\nu)\mathbb{I}+\nu\cos\frac{\theta}{2}\left(|S_+\rangle\langle(-)S|+|(-)S\rangle\langle S_+|\right)\right], \tag{37c}$$

and $V=(\mu_S-\mu_D)$ voltage applied to the QPC, $\mathcal{T}=\sqrt{4\pi g_S g_D}T$ is the tunneling constant, $(T=T_{pq})$, and $\nu=\sqrt{4\pi g_S g_D}\chi$ is the tunneling constant which depends on the occupation of the right QD $(\chi=\chi_{pq})$. g_i is the density of states of lead $i=S,D$, while Δ is the energy difference between states $|S_-\rangle$ and $|(-)S\rangle$.

Phonon influence on the QPC measurement of singlet-triplet qubits [H4]. The electron-phonon interaction Hamiltonian is given by the Hamiltonian (**??**). In this case, it is the real transitions between double QD state which are of interest. Hence, the evolution may be described using the Lindblad equation, similarly as for the electrons tunneling through the QPC.

Including the electron-phonon interaction requires adding an additional part to the Lindblad master equation (36). This is

$$\mathcal{L}_{ph}(t)=\frac{1}{\hbar^2}\left(\sum_i^4\frac{1}{2}(B_i^\dagger B_i\rho+\rho B_i^\dagger B_i)+\sum_i^4 B_i\rho B_i^\dagger\right). \tag{38}$$

The phonon Lindblad operators are of the form

$$B_1 = \sqrt{\gamma_{02}}|S_-\rangle\langle(-)S|, \tag{39a}$$

$$B_2 = \sqrt{\gamma_{20}}|(-)S\rangle\langle S_-| = \sqrt{\gamma_{02}e^{-(U+J)/k_BT}}|(-)S\rangle\langle S_-|, \tag{39b}$$

$$B_3 = \sqrt{\gamma_{12}}|S_+\rangle\langle(-)S| = \sqrt{\gamma_{21}\ e^{-J/k_BT}}|S_+\rangle\langle(-)S|, \tag{39c}$$

$$B_4 = \sqrt{\gamma_{21}}|(-)S\rangle\langle S_+|, \tag{39d}$$

where the transition rates are found using Fermi's golden rule and are given by $\gamma_{ij}=2\pi R_{ij}(\omega_{ij})$, where $\hbar\omega_{ij}$ is the energy difference between the two states corresponding to the transition described by the given Lindblad operator. The relevant spectral densities are given in Ref. [H1]. At zero temperature, phonons induce transitions only from higher energy states to lower energy states so $\gamma_{20}=\gamma_{12}=0$

The time evolution of the double QD system averaged over all possible single measurement runs is found by solving the above generalized master equation. Yet modern experimental techniques allow one to observe single system evolutions[80, 79, 83] which cannot be reproduced by this approach. To describe such single runs, probabilistic elements need to be introduced into the evolution following Refs [84, 26, 85, 86, 57, 74, 87].

The results presented are taken in the zero temperature limit which corresponds to experimental realizations of QPC measurements typically performed at temperatures that do not exceed 0.1 K, leading to extremely low phonon transition rates from lower to higher energy states. Fig. 11 shows exemplary time evolutions of the probability of finding the double QD in a spin-singlet state (green, dashed lines) or a spin-triplet state (red, solid) for an initial equal superposition of any triplet state and the singlet state $\frac{1}{\sqrt{2}}(|\uparrow\downarrow\rangle-|\downarrow\uparrow\rangle)$. The top panels show instances where the final state is a spin-triplet (the measurement outcome was the triplet state), while the bottom-panel evolutions ended up in the spin-singlet state (the measurement outcome was the singlet state). The electron-phonon interaction is included only in the right

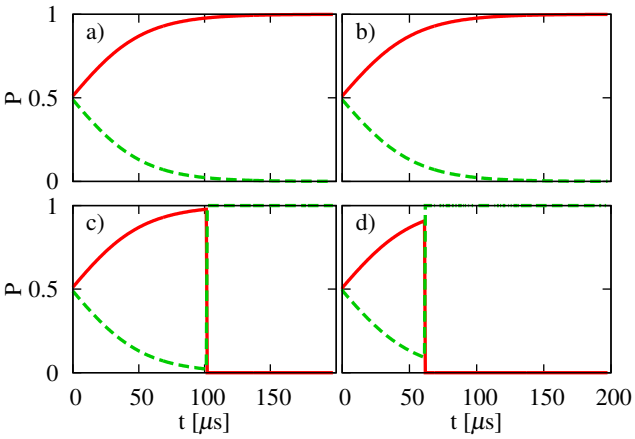

Figure 11: Exemplary singlet (green, dashed) and triplet (red, solid) probability time-evolutions for final triplet (a, b) and singlet (c, d) states, without (a, c) and with the phonon interaction (b, d).

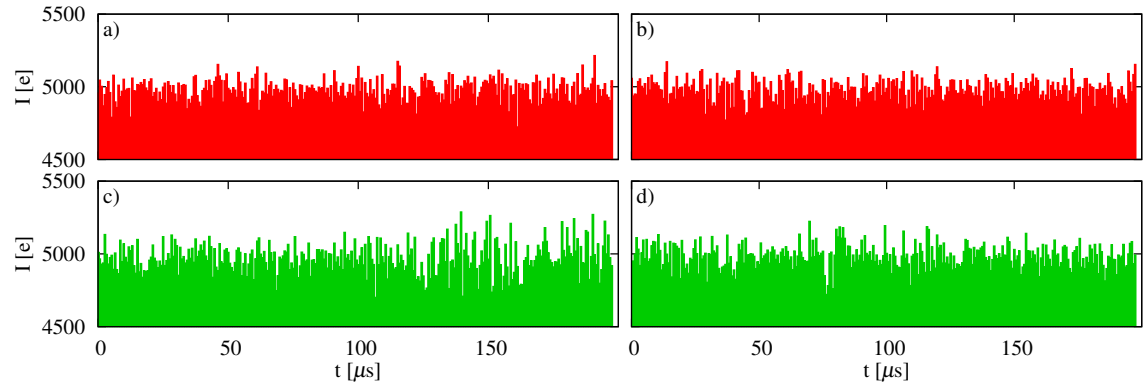

Figure 12: QPC current as a histogram of tunneling events for triplet (a, b) and singlet (c, d) states, without (a, c) and with the phonon interaction (b, d). The time interval used for the histogram is 0.66 μs.

panels; the phonon influence on coherence and localization is studied in more detail later on. As seen, regardless of the presence of the electron-phonon coupling, the continuous evolution leads to double QD localization in the triplet spin state (see Fig. 11 a, b), while for there to be a measurement of a singlet spin state, the occurrence of a quantum jump is required.

The simulation results for the QPC currents corresponding to the final singlet and triplet states are shown in Fig. 12. Even through the evolutions depicted in Fig. 11 show no clear difference between the phonon and no-phonon cases, in the phonon-free situation in Fig. 12 (left panels) a difference in the magnitude of the current fluctuations (noise) can be seen between the singlet and triplet case, while no such distinction is evident in the current when the phonon influence is included. For the realistic choice of material parameters, QPC and double QD properties, and for our choice of counting time step, the differences are relatively small, but still a period of time (after about 110 microseconds) when the double QD electrons occupy higher energy singlet states resulting in increased current fluctuations can be seen (Fig. 12 c). When the phonon coupling is included (Fig. 12 b, d) this distinction is diminished (to the level that no time period of increased fluctuations can be seen with the "bare eye"), so the measurement effect is suppressed.

Clearly, such observations based on the informal analysis of the current noise trace are to a large extent subjective and cannot form the base for rigorous conclusions on the measurement outcome or for assessing the role of phonon-induced dissipation. In order to provide a firm ground for such a discussion, the dependence of the Fano factoro [88, 89], which is defined as the zero frequency noise power divided by the noise power corresponding to a given mean current for Poissonian noise, is studied as a function of the relative strength of the electron-phonon

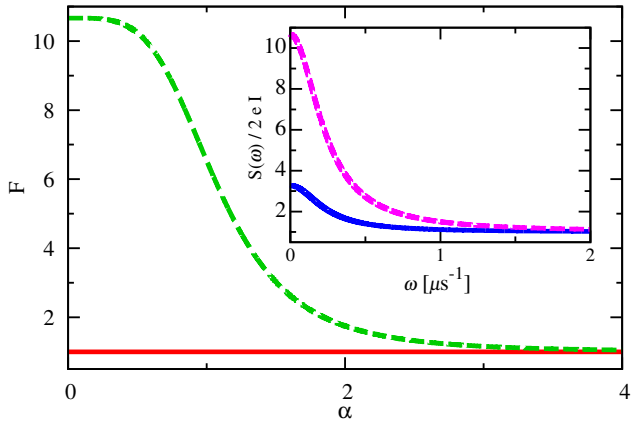

Figure 13: Steady state Fano factor for the QPC current as a function of the relative strength of the electron-phonon interaction for singlet (green dashed line) and triplet states (red solid). Inset: Normalized singlet steady state noise power spectra of the QPC detector current without (violet dashed line) and with electron-phonon interaction (blue solid), $\alpha = 1.5$.

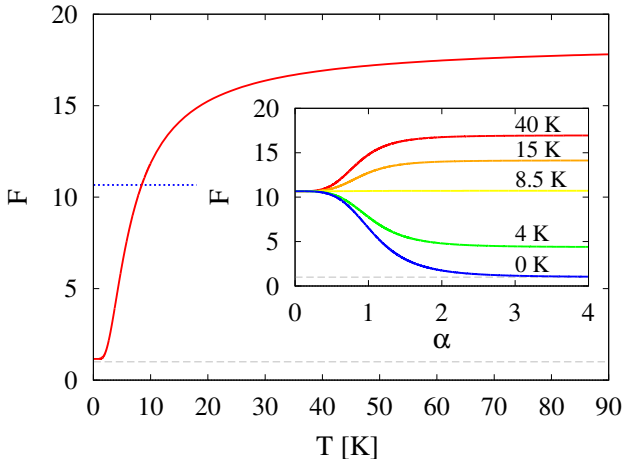

Figure 14: The Fano factor for a relatively strong electron phonon-interaction, $\alpha = 3$, as a function of temperature (red, solid line); no-phonon Fano factor (blue, dotted line). Inset: The Fano factor as a function of the strength of the electron-phonon interaction relative to the double QD-QPC interaction, α, for different temperatures. In both plots, the dashed grey line is set at Fano factor equal to one (Poissonian noise).

and double QD-QPC interactions.

Fig. 13 shows the singlet and triplet Fano factor curves as a function of the relative coupling strengths of the double QD to the phonon reservoir and to the QPC. For the sake of realism it is the tunneling parameters of the QPC which are changed, while the electron-phonon interaction is kept at a value corresponding to realistic gate defined QDs. The scaling parameter $\alpha = \frac{\mathcal{T}_0}{\mathcal{T}} = \frac{\nu_0}{\nu}$, with $\mathcal{T}_0 = 0.1$ and $\nu_0 = 2.25{\cdot}10^{-3}$, is chosen in such way that $\alpha = 1$ corresponds to the situation when the interaction with phonons is roughly the same strength as the interaction with the QPC; this means that $\sqrt{\gamma_{02}} = \nu_0\sqrt{V/\hbar}$. As can be seen, the phonons dominate at large α (small QPC current) leading to a suppression of the noise difference and breaking of the measurement scheme, while for large currents their effect is negligible. Note that the results discussed earlier correspond to the QPC interaction strength $\alpha = 2.5$. Even though the phonon-induced suppression of the spin-singlet Fano factor at this moderate value of the scaling parameter is small, the effects seen in Fig. 11 are already non-negligible.

Decoherence enhanced quantum measurement [H7] Fig. 14 shows the dependence of the singlet Fano factor as a function of temperature for relatively strong electron-phonon interaction at $\alpha = 3$; Fano factor equal to one corresponding to the triplet state is marked by the dashed grey line. Although at $T = 0$ phonons of such strength completely destroy the distinguishability of the singlet and triplet state via QPC current noise (both singlet and triplet Fano factors are equal to one), this is remedied already by a slight increase of the temperature. At $T = 8.5$ K, the redistribution of the different singlet occupations is strong enough to restore the Fano factor to the no-phonon value found (the no-phonon value of the Fano factor is marked by the blue, dotted line). This is due to the rising importance of phonon-induced transitions to higher energy, doubly occupied states which compensate for the transitions to the lower energy, singly occupied state. Further increasing the temperature leads to an enhancement of

the Fano factor beyond the no-phonon value. The effect of temperature is strong between 0 and 20 K, and then starts to slowly saturate, yielding already ample enhancement of the Fano factor by 15 K, long before the excited QD states need to be taken into account.

This is further quantified in the inset of the figure where the Fano factor is plotted as a function of the scaling parameter α, which is inversely proportional to the strength of the double QD-QPC interaction, at different temperatures. Regardless of the temperature, phonon effects are negligible when the double QD-QPC interaction dominates, near $\alpha = 0$. Their importance rises quickly, when the interactions become comparable, and then saturates slowly after the interaction with phonons becomes twice as strong as the interaction with the QPC. Hence, the interaction with phonons is relevant when the QPC is coupled weakly to the double QD, and may serve to increase the effectiveness of the measurement in this situation.

At high enough temperatures, the electron-phonon interaction will cause transitions to excited QD states. This will lead to double occupations in the triplet subspace in the situation when one of the electrons is in the QD ground state, and the other is in the QD excited state. The occurrence of transitions to such states will lead to fluctuations of the QPC current noise, which will also become super-Poissonian. Although at not extremely high temperatures this super-Poissonian character will be much weaker than in the singlet case, it could complicate data interpretation. However, since the dependence on temperature is strong only for relatively small temperatures, the high temperature range is of no experimental interest.

4.3.7 Summary

A series of papers titled "The impact of the environment on the coherence and quantum correlations of quantum dot ensembles" constitute the scientific achievement described above. The series consists of eight articles, in which a diverse collection of problems involving spin and charge states confined in quantum dots interacting with a phonon environment and a nuclear environment has been considered. The two types of interactions have been studied because they constitute the two basic quantum sources of decoherence in quantum dot qubits. The predominance of a given decoherence type is dependent on the type of the qubit studied, and is important since they lead to qualitatively different evolutions of qubit coherence, interqubit entanglement, or interqubit quantum discord, as well as different methods to prevent decoherence or utilize it.

In articles [H2, H3, H8] we studied phonon-induced decoherence of excitonic qubits. Such decoherence leads to a characteristic partial pure dephasing which is the result of non-Markovian processes. In articles [H1, H4, H7] we found and studied in the context of quantum measurement a class of single- and two-phonon processes which lead to pure dephasing (two-phonon processes) and relaxation (single-phonon processses) of singlet-triplet spin qubits. The two-phonon pure dephasing is unavoidable since it persists even at very low temparatures. In the remaining two papers, [H5, H6], we studied the decoherence of single-spin qubits resulting from the hyperfine interaction between the electron spin (qubit) and the spins of the nuclei of the surrounding atoms. Such decoherence is not of strictly pure dephasing character.

In term of the studied problems, the articles have to be divided in a different manner. The papers [H2, H4, H5, H6, H7, H8] are all related to the subject of quantum measurements. In article [H2] we have shown what can be learned about two-qubit entanglement in the situation when a limited information about the system state can be acquired (the number of density matrix elements which can be measured is limited). In articles [H4, H7] we have studied the effect of decoherence on the measurement process itself and we found a way of utilizing decoherence to enhance the distinguishability between measurement outcomes. In articles [H5, H6] we have shown how to use the decay of quantum correlations to measure external magnetic fields. In the paper [H8] we have in turn shown how to use quantum measurements to prevent decoherence. In articles [H2, H5] we studied the decay of the type of quantum correlations that are described by entanglement, while in articles [H3, H6] we studied the type

of quantum correlations described by the quantum discord. In the article [90] a phonon-induced decoherence mechanism for spin states has been found which cannot be prevented by the right choice of material parameters or lowering the temperature. In the article [H7], on the other hand, we found a situation for which the presence of decoherence has a constructive effect on a measurement process.

As can be seen, the papers of the scientific achievement constitute a coherent collection, despite their diversity. The experiences related to the study of different phenomena led to a better understanding of the physics and processes which lead to decoherence, the decay of quantum correlations. This in turn allowed for us to find methods to utilize and prevent decoherence.

References

[1] L. Jacak, P. Hawrylak, and A. Wojs, *Quantum Dots* (Springer Verlag, Berlin, 1998).

[2] *Quantum Dots: Research Developments*, edited by P. A. Ling (Nova Science, NY, 2005).

[3] M. Kroutvar, Y. Ducommun, D. Heiss, M. Bichler, D. Schuh, G. Abstreiter, and J. J. Finley, Nature **432**, 81 (2004).

[4] A. Greilich, M. Schwab, T. Berstermann, T. Auer, R. Oulton, D. R. Yakovlev, M. Bayer, V. Stavarache, D. Reuter, and A. Wieck, Phys. Rev. B **73**, 045323 (2006).

[5] N. Y. Kim, K. Kusudo, C. Wu, N. Masumoto, A. Loffler, S. Hofling, N. Kumada, L. Worschech, A. Forchel, and Y. Yamamoto, Nature Physics **7**, 681 (2011).

[6] J. M. Elzerman, R. Hanson, L. H. Willems van Beveren, B. Witkamp, L. M. K. Vandersypen, and L. P. Kouwenhoven, Nature **430**, 431 (2004).

[7] R. Hanson, L. H. W. van Beveren, I. T. Vink, J. M. Elzerman, W. J. M. Naber, F. H. L. Koppens, L. P. Kouwenhoven, and L. M. K. Vandersypen, Phys. Rev. Lett. **94**, 196802 (2005).

[8] J. R. Petta, A. C. Johnson, J. M. Taylor, E. A. Laird, A. Yacoby, M. D. Lukin, C. M. Marcus, M. P. Hanson, and A. C. Gossard, Science **309**, 2180 (2005).

[9] P. Zanardi and F. Rossi, Phys. Rev. Lett. **81**, 4752 (1998).

[10] D. Loss and D. P. DiVincenzo, Phys. Rev. A **57**, 120 (1998).

[11] P. Borri, W. Langbein, S. Schneider, U. Woggon, R. L. Sellin, D. Ouyang, and D. Bimberg, Phys. Rev. Lett. **87**, 157401 (2001).

[12] A. Vagov, V. M. Axt, and T. Kuhn, Phys. Rev. B **67**, 115338 (2003).

[13] A. Vagov, V. M. Axt, T. Kuhn, W. Langbein, P. Borri, and U. Woggon, Phys. Rev. B **70**, 201305(R) (2004).

[14] V. N. Golovach, A. Khaetskii, and D. Loss, Phys. Rev. Lett. **93**, 016601 (2004).

[15] A. V. Khaetskii and Y. V. Nazarov, Phys. Rev. B **64**, 125316 (2001).

[16] J. I. Climente, A. Bertoni, G. Goldoni, M. Rontani, and E. Molinari, Phys. Rev. B **75**, 081303(R) (2007).

[17] J. I. Climente, A. Bertoni, G. Goldoni, M. Rontani, and E. Molinari, Phys. Rev. B **76**, 085305 (2007).

[18] K. Shen and M. W. Wu, Phys. Rev. B **76**, 235313 (2007).

[19] V. N. Golovach, A. Khaetskii, and D. Loss, Phys. Rev. B **77**, 045328 (2008).

[20] A. Grodecka, P. Machnikowski, and J. Förstner, Phys. Rev. B **78**, 085302 (2008).

[21] E. A. Muljarov and R. Zimmermann, Phys. Rev. Lett. **93**, 237401 (2004).

[22] E. A. Muljarov, T. Takagahara, and R. Zimmermann, Phys. Rev. Lett. **95**, 177405 (2005).

[23] K. Hornberger and J. E. Sipe, Phys. Rev. A **68**, 012105 (2003).

[24] P. Machnikowski, Phys. Rev. Lett. **96**, 140405 (2006).

[25] G. D. Mahan, in *Polarons in Ionic Crystals and Polar Semiconductors*, edited by J. T. Devreese (North-Holland, Amsterdam, 1972).

[26] H.-P. Breuer and F. Petruccione, *The Theory of Open Quantum Systems* (Oxford University Press, Oxford, 2002).

[27] F. H. L. Koppens, C. Buizert, K. J. Tielrooij, I. T. Vink, K. C. Nowack, T. Meunier, L. P. Kouwenhoven, and L. M. K. Vandersypen, Nature **442**, 766 (2006).

[28] W. A. Coish and J. Baugh, Phys. Stat. Sol. B **246**, 2203 (2009).

[29] W. A. Coish, J. Fischer, and D. Loss, PHYSRB **81**, 165315 (2010).

[30] Ł. Cywiński, Acta Phys. Pol. A **119**, 576 (2011).

[31] A. Abragam, *The Principles of Nuclear Magnetism* (Oxford University Press, New York, 1983).

[32] I. A. Merkulov, A. L. Efros, and M. Rosen, PHYSRB **65**, 205309 (2002).

[33] E. Barnes, Ł. Cywiński, and S. Das Sarma, PHYSRB **84**, 155315 (2011).

[34] Ł. Cywiński, W. M. Witzel, and S. Das Sarma, PHYSRB **79**, 245314 (2009).

[35] A. Einstein, B. Podolsky, and N.Rosen, Phys. Rev. **47**, 777 (1935).

[36] E. Schrödinger, Proc. Cambridge Philos. Soc. **31**, 555 (1935).

[37] J. S. Bell, Physics **1**, 195 (1964).

[38] M. A. Nielsen and I. L. Chuang, *Quantum Computation and Quantum Information* (Cambridge University Press, Cambridge, 2000).

[39] C. H. Bennett, G. Brassard, C. Crépeau, R. Jozsa, A. Peres, and W. K. Wootters, Phys. Rev. Lett. **70**, 1895 (1993).

[40] C. H. Bennett and S. J. Wiesner, Phys. Rev. Lett. **69**, 2881 (1992).

[41] A. K. Ekert, Phys. Rev. Lett. **67**, 661 (1991).

[42] T. Yu and J. H. Eberly, Phys. Rev. B **66**, 193306 (2002).

[43] T. Yu and J. H. Eberly, Phys. Rev. B **68**, 165322 (2003).

[44] T. Yu and J. H. Eberly, Phys. Rev. Lett. **93**, 140404 (2004).

[45] P. J. Dodd and J. J. Halliwell, Phys. Rev. A **69**, 052105 (2004).

[46] M. Horodecki, P. Horodecki, and R. Horodecki, Phys. Rev. Lett. **78**, 574 (1997).

[47] C. H. Bennett, H. J. Bernstein, S. Popescu, and B. Schumacher, Phys. Rev. A **53**, 2046 (1996).

[48] C. H. Bennett, G. Brassard, S. Popescu, B. Schumacher, J. A. Smolin, and W. K. Wootters, Phys. Rev. Lett. **76**, 722 (1996).

[49] C. H. Bennett, D. P. DiVincenzo, J. A. Smolin, and W. K. Wootters, Phys. Rev. A **54**, 3824 (1996).

[50] A. Peres, Phys. Rev. Lett. **77**, 1413 (1996).

[51] M. Horodecki, P. Horodecki, and R. Horodecki, Phys. Lett. A **223**, 1 (1996).

[52] S. Hill and W. K. Wootters, Phys. Rev. Lett. **78**, 5022 (1997).

[53] W. K. Wootters, Phys. Rev. Lett. **80**, 2245 (1998).

[54] B. Krummheuer, V. M. Axt, and T. Kuhn, Phys. Rev. B **65**, 195313 (2002).

[55] E. Biolatti, R. C. Iotti, P. Zanardi, and F. Rossi, Phys. Rev. Lett. **85**, 5647 (2000).

[56] E. Pazy, E. Biolatti, T. Calarco, I. D'Amico, P. Zanardi, F. Rossi, and P. Zoller, Europhys. Lett. **62**, 175 (2003).

[57] T. M. Stace, S. D. Barrett, H.-S. Goan, and G. J. Milburn, Phys. Rev. B **70**, 205342 (2004).

[58] T. M. Stace and S. D. Barrett, Phys. Rev. Lett. **92**, 136802 (2004).

[59] H. Olliver and W. Żurek, Phys. Rev. Lett. **88**, 017901 (2001).

[60] L. Henderson and V. Vedral, Journal of Physics A: Mathematical and General **34**, 6899 (2001).

[61] A. Ferraro, L. Aolita, D. Cavalcanti, F. M. Cucchietti, and A. Acín, Phys. Rev. A **81**, 052318 (2010).

[62] E. Knill and R. Laflamme, Phys. Rev. Lett. **81**, 5672 (1998).

[63] B. Meurer, D. Heitmann, and K. Ploog, Phys. Rev. Lett. **68**, 1371 (1992).

[64] G. Passante, O. Moussa, D. A. Trottier, and R. Laflamme, Phys. Rev. A **84**, 044302 (2011).

[65] C. Silberhorn, Physics **6**, 132 (2013).

[66] L. Mazzola, J. Piilo, and S. Maniscalco, Phys. Rev. Lett. **104**, 200401 (2010).

[67] B. Dakić, V. Vedral, and Č. Brukner, Phys. Rev. Lett. **105**, 190502 (2010).

[68] A. Miranowicz, P. Horodecki, R. W. Chhajlany, J. Tuziemski, and J. Sperling, Phys. Rev. A **86**, 042123 (2012).

[69] P. Blanchard, L. Jakóbczyk, and R. Olkiewicz, Phys. Lett. A **208**, 7 (2001).

[70] M. Piani, Phys. Rev. A **86**, 034101 (2012).

[71] T. Tufarelli, D. Girolami, R. Vasile, S. Bose, and G. Adesso, Phys. Rev. A **86**, 052326 (2012).

[72] T. Tufarelli, T. MacLean, D. Girolami, R. Vasile, and G. Adesso, J. Phys. A **46**, 275308 (2013).

[73] C. Beenakker and H. van Houten, Solid State Physics **44**, 1 (1991).

[74] S. D. Barrett and T. M. Stace, Phys. Rev. B **73**, 075324 (2006).

[75] D. V. Averin and E. V. Sukhorukov, Phys. Rev. Lett. **95**, 126803 (2005).

[76] T. Meunier, I. T. Vink, L. H. W. van Beveren, F. H. L. Koppens, H. P. Tranitz, W. Wegscheider, L. P. Kouwenhoven, and L. M. K. Vandersypen, Phys. Rev. B **74**, 195303 (2006).

[77] M. C. Rogge, B. Harke, C. Fricke, F. Hohls, M. Reinwald, W. Wegscheider, and R. J. Haug, Phys. Rev. B **72**, 233402 (2005).

[78] C. Barthel, D. J. Reilly, C. M. Marcus, M. P. Hanson, and A. C. Gossard, Phys. Rev. Lett. **103**, 160503 (2009).

[79] M. C. Cassidy, A. S. Dzurak, R. G. Clark, K. D. Petersson, I. Farrer, D. A. Ritchie, and C. G. Smith, Appl. Phys. Lett. **91**, 222104 (2007).

[80] J. Bylander, T. Duty, and P. P.Delsing, Nature **434**, 361 (2005).

[81] Ł. Marcinowski, M. Krzyżosiak, K. Roszak, P. Machnikowski, R. Buczko, and J. Mostowski, Acta Phys. Pol. A **119**, 640 (2011).

[82] S. A. Gurvitz and Y. S. Prager, Phys. Rev. B **53**, 15932 (1996).

[83] S. Gustavsson, I. Shorubalko, R. Leturcq, S. SchĂśn, and K. Ensslin, Appl. Phys. Lett. **92**, 152101 (2008).

[84] P. Meystre and M. Sargent, *Elements of Quantum Optics* (Springer-Verlag, Berlin, 2007).

[85] H.-S. Goan and G. J. Milburn, Phys. Rev. B **64**, 235307 (2001).

[86] H.-S. Goan, G. J. Milburn, H. M. Wiseman, and H. Bi Sun, Phys. Rev. B **63**, 125326 (2001).

[87] H. M. Wiseman, D. W. Utami, H. B. Sun, G. J. Milburn, B. E. Kane, A. Dzurak, and R. G. Clark, Phys. Rev. B **63**, 235308 (2001).

[88] U. Fano, Phys. Rev. **72**, 26 (1947).

[89] Y. M. Blanter and M. Büttiker, Physics Reports **336**, 1 (2000).

[90] K. Roszak and P. Machnikowski, Phys. Rev. B **80**, 195315 (2009).

5 Description of other scientific achievements

5.1 Bibliometric data (from the 8th of September 2015)

No. of published scientific papers: 29
No. of citations: 215
No. of citations without self-citations: 175
Cumulative impact factor (according to JCR): 48.963
Hirscha index (according to Web of Science): 7

5.2 List of articles not included in the habilitation thesis

5.2.1 Before obtaining the PhD

[D1] K. Roszak, V. M. Axt, T. Kuhn, P. Machnikowski, *Exciton spin decay in quantum dots to bright and dark states*, Phys. Rev. B **76** (2007) 195324.

[D2] K. Roszak, P. Machnikowski, L. Jacak, *Decay of entanglement due to pure dephasing: the role of geometry of entangled states*, Open Sys. Inf. Dyn. **14** (2007) 63.

[D3] K. Roszak, P. Machnikowski, *Complete disentanglement by partial pure dephasing*, Phys. Rev. A **73** (2006) 022313.

[D4] K. Roszak, P. Machnikowski, *"Which path" decoherence in quantum dot experiments*, Phys. Lett. A **351** (2006) 251-256.

[D5] K. Roszak, P. Machnikowski, L. Jacak, *Phonon-induced disentanglement of confined excitons*, Phys. Stat. Sol. (b) **243** (2006) 2261.

[D6] K. Roszak, P. Machnikowski, L. Jacak, *Phonon-induced dephasing in quantum dots - interpretation in terms of information leakage*, Acta Phys. Pol. A **110** (2006) 325.

[D7] K. Roszak, P. Machnikowski, L. Jacak, *Complete and partial loss of entanglement due to a phonon-assisted dephasing process*, Acta Phys. Pol. A **110** (2006) 331.

[D8] K. Roszak, A. Grodecka, P. Machnikowski, T. Kuhn, *Phonon-induced decoherence for a quantum dot spin qubit operated by Raman passage*, Phys. Rev. B **71** (2005) 195333?1-17.

Review chapters:

[D9] A. Grodecka, L. Jacak, P. Machnikowski, K. Roszak, *Phonon impact on the coherent control of quantum states in semiconductor quantum dots*, w: Quantum Dots: Research Developments, ed. P. A. Ling, Nova Science Publishers, New York, 2005, pp. 47-88.

Published conference presentations:

[D10] K. Roszak, P. Machnikowski, L. Jacak, *"Which way" interpretation of the dephasing of charge qubits in quantum dots*, J. Phys. Conf. Series **30** (2006) 52-55.

5.2.2 After obtaining the PhD (articles not included in the habilitation)

[E1] K. Roszak, Ł. Cywiński, *Characterization and measurement of qubit-environment entanglement generation during pure dephasing*, Phys. Rev. A **92** (2015) 032310.

[E2] N. Ubbelohde, K. Roszak, F. Hohls, N. Maire,R. J. Haug, T. Novotný, *Strong quantum memory at resonant Fermi edges revealed by shot noise*, Scientific Reports **2** (2012) 374.

[E3] K. Roszak, T. Novotný, *Non-Markovian effects at the Fermi-edge singularity in quantum dots*, Physica Scripta **T151** (2012) 014053.

[E4] Ł. Marcinowski, M. Krzyżosiak, K. Roszak, P. Machnikowski, *Phonon effects on the weak measurement of charge states in quantum dots with a quantum point contact*, Acta Phys. Pol. A **119** (2011) 640-643.

[E5] P. Machnikowski, K. Roszak, A. Sitek, *Collective luminescence and phonon induced processes in double quantum dots*, Acta Phys. Pol. **116** (2009) 818.

[E6] Ł. Marcinowski, K. Roszak, P. Machnikowski, *Singlet-triplet dephasing in asymmetric quantum dot molecules*, Acta Phys. Pol. **116** (2009) 874.

[E7] K. Roszak, P. Machnikowski, *Phonon induced pure dephasing of two electron spin states in vertical quantum dot molecules*, Acta Phys. Pol. **116** (2009) 877.

[E8] K. Roszak, P. Machnikowski, V. M. Axt, T. Kuhn, *Exciton spin decay in quantum dots: single and double phonon assisted transitions*, Phys. Stat. Sol. (c) **6** (2009) 537.

[E9] K. Roszak, P. Machnikowski, V.M. Axt, T. Kuhn, *One and two phonon assisted transitions between exciton spin states in a quantum dot*, Acta Phys. Pol. **114** (2008) 1329.

Unpublished papers avaliable on the archive:

[E10] K. Roszak, Ł. Cywiński, *The relation between the quantum discord and quantum teleportation: the physical interpretation of the transition point between different quantum discord decay regimes*, arXiv:1505.05741 (2015).

Rewiev chapters:

[E11] P. Karwat, K. Gawarecki, K. Roszak, A. Sitek, P. Machnikowski, *Phonon-assisted processes and spontaneous emission in double quantum dots*, w: Quantum Dot Molecules, ed. J. Wu, Z. M. Wang , Springer New York, New York, 2014, pp. 281-331.

Published conference presentations:

[E12] N. Ubbelohde, K. Roszak, F. Hohls, N. Maire,R. J. Haug, T. Novotný, *Shot-Noise at a Fermi-Edge Singularity: Non-Markovian Dynamics*, AIP Conf. Proc **1566** (2013) pp. 225-226.

[E13] K. Roszak, P. Machnikowski, V. M. Axt, T. Kuhn, *Spin decoherence of a confined exciton due to one- and two-phonon assisted transitions*, AIP Conf. Proc. **1199** (2010) pp. 413-414.

5.3 Description of the research conducted before obtaining the PhD

I began to conduct research before starting PhD studies with the analysis of phonon induced decoherence in single qubit gates preformed via the STIRAP procedure [D8]. This involved studies of the errors which occur in the gate operation due to the interaction with the environment. The main result of the article was identifying the parameter ranges for which the errors are reduced.

With the beginning of the PhD studies I continued to study the interaction of QDs with the surrounding crystal lattice, both in the context of quantum information theory and in the context of the study of quantum open systems. Using the example of a single QD for which phonon-induced effects lead to partial pure dephasing, I have shown that the decoherence may be qualitatively and quantitatively interpreted in terms of information transfer between the QD and the environment [D4]. A system of two QDs allowed me to study the decay of entanglement during partial pure dephasing and to observe the differences in entanglement decay in the regimes of a common environment and separable environments. It turned out that sudden death of entanglement is only possible for a certain class of initial entangled states under this type of interaction [D3].

The interaction between spins confined in QDs with phonons is indirect and is only possible when the electron-phonon interaction is supplemented witha an interaction that mixes spin and orbital degrees of freedom. This is the case for excitonic spin, when interplay of the Bir-Pikus Hamiltonian and the short-range exchange interaction lead to the relaxation of a bright excitonic state to dark states, which is an order of magnitude faster than other relaxation mechanisms present in the system [D1].

5.4 Description of the research conducted after obtaining the PhD, which is not included in the habilitation

The article [E2] contains an experimental and theoretical description of the current noise through a single QD in the Fermi edge singularity regime. The description of the noise is impossible using the Markov approximation, but non-Markovian theory gives a very good agreement with the experimental data. A detailed theoretical study of this effect in different parameter ranges is the topis of Ref. [E3].

My current studies remain on the border between QD physics and quantum information theory. Ref. [E10] contains a physical interpretation of the transition between regimes of quantum and classical decohrence characteristic of the quantum discord. This is possible using the minimal (maximal) teleportation fidelity when a qubit is teleported via a mixed state. It turns out that the state which is hardest (easiest) to teleport changes at exactly the same parameter values at which the transition between different discord decoherence regimes is observed.

Ref. [E1] contains the answer to the question, when entanglement between a qubit and its environment is formed under an evolution which leads to pure dephasing of the qubit. Additionally, it was possible to show that for a large range of initial states of the environment, it is possible to detect the entanglement by performing measurements on the environment alone.

5.5 Awards

2006 DAAD Scholarship for Young Scientists
2009 Award of the Prime Minister of the PhD Thesis
2009 Award of the Rektor of the Wrocław University of Technology
2011 START Scholarship of the Foundation for Polish Science
2012 Chosen to take part in the Lindau Nobel Laureate Meeting
(via the Foundation For Polish Science)

5.6 Head Investigator in the following grants

- NCN (Narodowe Centrum Nauki) Research Project no 2012/05/B/ST3/02875
Kwantowe efekty pomiaru w układach kropek kwantowych
Institute of Physics, Wrocław University of Technology, 2012-2015

5.7 Participation in research projects

Current projects:

- NCN (Narodowe Centrum Nauki) Research Project no 2012/07/B/ST3/03616
Dynamika splątania zlokalizowanych spinów w półprzewodnikach z zastosowaniem do spektroskopii szumu środowiskowego
Institute of Physics, Polish Academy of Sciences, 2013-2016
- Principal Investigator

- NCN (Narodowe Centrum Nauki) Research Project no 2011/01/B/ST2/05459
Wrażliwosc skorelowanych ukżadow kropek kwantowych na zewnętrzne pole magnetyczne wywołana oddziaływaniem z otoczeniem
Department of Theoretical Physics and Quantum Information, Gdańsk University of Technology, 2011-2015
- Principal Investigator

Concluded projects:

- NCN (Narodowe Centrum Nauki) Research Project no 2011/01/B/ST3/02415
  Kolektywna luminescencja kropek kwantowych
  Institute of Physics, Wrocław University of Technology,, 2011-2014
  - Principal Investigator

- Project TEAM of the Foundation for Polish Science (TEAM/2009-4/7)
  Semiconductor nanostructures for renewable energy, information processing and communication technologies
  Institute of Physics, Wrocław University of Technology, 2010-2014
  - Investigator

- Research Group Linkage Grant of the Alexander von Humboldt Foundation
  Optical properties, quantum optical control and dephasing in semiconductor nanostructures
  Institute of Physics, Wrocław University of Technology, 2010-2012
  - Investigator

- Research Project 202/07.J051 (Bilateral Czech-German Grant)
  Full counting statistics in non-markovian nano-systems
  Department of Solid State Physics, Charles University in Prague, 2009-2010
  - Investigator

- Research Grant N N202 1336 33
  Ultraszybka kinetyka i nieliniowa odpowiedź optyczna niskowymiarowych struktur półprzewodnikowych: podwójnych kropek i studni kwantowych
  Institute of Physics, Wrocław University of Technology, 2007-2009
  - Investigator

5.8 Invited conference talks

1. K. Roszak, P. Machnikowski
   Phonon induced decoherence of two-electron spin states in a double quantum dot
   Nonequilibrium Nanostructures, International Workshop, Drezden, Germany (2008)

2. K. Roszak, P. Machnikowski, P. Horodecki, R. Horodecki
   Entanglement measurement in dephased systems
   Sympozjum KCIK, Sopot (2010)

3. K. Roszak, P. Mazurek, R. W. Chhajlany, and P. Horodecki
   Magnetic field dependence of quantum dot spin qubit entanglement decay
   EMN Fall, Orlando, USA (2013)

5.9 Other conference talks

- The 9th International School on Theoretical Physics: Symmetry and Structural Properties of Condensed Matter (Myczkowce 2005)

- "Jaszowiec" International School and Conference on the Physics of Semiconductors (Jaszowiec 2006)

- International Workshop on the Optical Properties of Nanostructures (Münster, Germany 2012)

- "Jaszowiec" International School and Conference on the Physics of Semiconductors (Wisła 2013)

- International Conference of Theoretical Physics: Coherence and Correlations in nanosystems (Ustroń 2014)

6 International and national collaboration

1. Institut für Festkörpertheorie, Westfalische Wilhelms-Universtät Münster, Niemcy
   - prof. Tilmann Kuhn - 2 publications
2. National Quantum Information Centre of Gdańsk
   - prof. Ryszard Horodecki - 1 publication
   - prof. Paweł Horodecki - 4 publications, research project
3. Physikalisches Institut, Universität Bayreuth, Germany
   - prof. Vollrath Martin Axt - 1 publication
4. Department of Solid State Physics, Charles University in Prague
   - dr Tomaš Novotný - 3 publications, research project
5. Department of Optics, Palacký University, Olomouc, Czech Republic
   - dr Radim Filip - 1 publication
6. Institute of Physics, Polish Academy of Sciences, Warsaw
   - dr Łukasz Cywiński - research project
7. NTH Nano, Leibniz Universtät Hannover
   - prof. Rolf Haug - 1 publication

Ł. Rosca